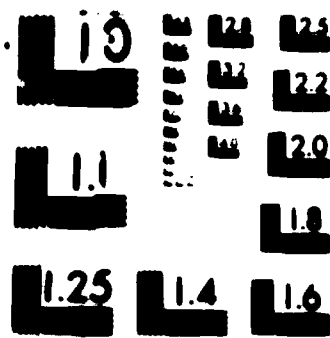


ESTIMATION OF EXTINCTION COEFFICIENTS AT 375 AND 1100
MICROMETERS FROM SA (U) NAVAL POSTGRADUATE SCHOOL
MONTEREY CA M GARCIA DE QUEVEDO MAR 87

MICROMETERS FROM SA (U) NAVAL POSTGRADUATE SCHOOL
MONTEREY CA M GARCIA DE QUEVEDO MAR 87

F/G 28/6

NL



NAVAL POSTGRADUATE SCHOOL

Monterey, California

AD-A181 461



DTIC
ELECTE
JUN 17 1987
S D E

THESIS

ESTIMATION OF EXTINCTION COEFFICIENTS
AT 3.75 AND 11.00 μm FROM SATELLITE
MEASUREMENTS AT 0.63 AND 0.86 μm

by

Margarita Garcia de Quevedo

March 1987

Thesis Advisor

P. A. Durkee

Approved for public release; distribution is unlimited.

A181461

REPORT DOCUMENTATION PAGE

1a REPORT SECURITY CLASSIFICATION UNCLASSIFIED		1b RESTRICTIVE MARKINGS	
2a SECURITY CLASSIFICATION AUTHORITY		3 DISTRIBUTION/AVAILABILITY OF REPORT Approved for public release; distribution is unlimited.	
2b DECLASSIFICATION/DOWNGRADING SCHEDULE		5 MONITORING ORGANIZATION REPORT NUMBER(S)	
4 PERFORMING ORGANIZATION REPORT NUMBER(S)		7a NAME OF MONITORING ORGANIZATION Naval Postgraduate School	
6a NAME OF PERFORMING ORGANIZATION Naval Postgraduate School	6b OFFICE SYMBOL (if applicable) 63	7b ADDRESS (City, State, and ZIP Code) Monterey, California 93943-5000	
8a NAME OF FUNDING/SPONSORING ORGANIZATION		9 PROCUREMENT INSTRUMENT IDENTIFICATION NUMBER	
8b OFFICE SYMBOL (if applicable)		10 SOURCE OF FUNDING NUMBERS	
8c ADDRESS (City, State, and ZIP Code) Monterey, California 93943-5000		PROGRAM ELEMENT NO	PROJECT NO
		TASK NO	WORK UNIT ACCESSION NO
11 TITLE (Include Security Classification) ESTIMATION OF EXTINCTION COEFFICIENTS AT 3.75 AND 11.00 μm FROM SATELLITE MEASUREMENTS AT 0.63 AND 0.86 μm			
12 PERSONAL AUTHOR(S) Garcia de Quevedo, Margarita, NMN			
13a TYPE OF REPORT Master's Thesis	13b TIME COVERED FROM TO	14 DATE OF REPORT (Year Month Day) 1987 March	15 PAGE COUNT 56
16 SUPPLEMENTARY NOTATION			
17 COSATI CODES		18 SUBJECT TERMS (Continue on reverse if necessary and identify by block number)	
FIELD	GROUP	SUB-GROUP	
		Visible and infrared, extinction, aerosols, satellite, techniques.	
19 ABSTRACT (Continue on reverse if necessary and identify by block number)			
A method for estimating extinction coefficients in the near-infrared and infrared wavelengths from satellite measurements in the visible was developed. Five tests were devised to examine the limits and sensitivity of the model. The first test studied the error inherent in the retrieval of the parameters which are needed to describe the distribution of atmospheric particles and are direct inputs for the calculation of extinction at 3.75 and 11.00 μm . Also studied were errors associated with uncertainties in the extinction values, uncertainties in relative humidity values, deviations of particle size distribution from the model and effects of high winds on the aerosol distribution. Results indicate that the biggest error results when wind generated aerosols change the particle size distribution especially at radii larger than 2 μm . The error reaches 82% for prediction at 11.00 μm .			
20 DISTRIBUTION/AVAILABILITY OF ABSTRACT <input checked="" type="checkbox"/> UNCLASSIFIED/UNLIMITED <input type="checkbox"/> SAME AS RPT <input type="checkbox"/> DTIC USERS		21 ABSTRACT SECURITY CLASSIFICATION UNCLASSIFIED	
22a NAME OF RESPONSIBLE INDIVIDUAL P. A. Durkee		22b TELEPHONE (Include Area Code) (408) 646-3465	22c OFFICE SYMBOL 63De

Keywords:

19 ABSTRACT (continued)

μm at 60% relative humidity. The smallest error, less than 7% for all variations, is associated with the retrieval technique itself. Errors up to 25% in the measured satellite extinction coefficients lead to errors of up to 25% in the estimated values for both the marine and rural models. Results indicate that the rural model at high values of relative humidity is affected the most with an error of 31% at a RH of 95% at 11.00 μm . Negative deviations in the marine particle size distribution give rise to large errors for $\lambda = 11.00 \mu\text{m}$. For 20% deviation, the error can be as high as 41%. The error decreases accordingly as the percent deviation is reduced.

Approved for public release; distribution is unlimited.

Estimation of Extinction Coefficients
at 3.75 and 11.00 μm from Satellite
Measurements at 0.63 and 0.86 μm

by

Margarita Garcia de Quevedo
Lieutenant, United States Navy
B.S., Texas A & M University, 1975
M.Ed., Texas A & M University, 1979

Submitted in partial fulfillment of the
requirements for the degree of

Accession For	
NTIS GRA&I	<input checked="" type="checkbox"/>
DTIC TAB	<input checked="" type="checkbox"/>
Unannounced	<input type="checkbox"/>
Justification	
By	
Distribution/	
Availability Codes	
Dist	Avail and/or Special
A-1	

MASTER OF SCIENCE IN METEOROLOGY AND OCEANOGRAPHY

from the

NAVAL POSTGRADUATE SCHOOL
March 1987



Author:

Margarita Garcia de Quevedo
Margarita Garcia de Quevedo

Approved by:

Paul A. Duckee
P. A. Duckee, Thesis Advisor

C. H. Wash
C. H. Wash, Second Reader

R. J. Renard
R. J. Renard, Chairman,
Department of Meteorology

G. E. Schacher
G. E. Schacher,
Dean of Science and Engineering

ABSTRACT

A method for estimating extinction coefficients in the near-infrared and infrared wavelengths from satellite measurements in the visible was developed. Five tests were devised to examine the limits and sensitivity of the model. The first test studied the error inherent in the retrieval of the parameters which are needed to describe the distribution of atmospheric particles and are direct inputs for the calculation of extinction at 3.75 and 11.00 μm . Also studied were errors associated with uncertainties in the extinction values, uncertainties in relative humidity values, deviations of particle size distribution from the model and effects of high winds on the aerosol distribution. Results indicate that the biggest error results when wind generated aerosols change the particle size distribution especially at radii larger than 2 μm . The error reaches 82% for prediction at 11.00 μm at 60% relative humidity. The smallest error, less than 7% for all variations, is associated with the retrieval technique itself. Errors up to 25% in the measured satellite extinction coefficients lead to errors of up to 25% in the estimated values for both the marine and rural models. Results indicate that the rural model at high values of relative humidity is affected the most with an error of 31% at a RH of 95% at 11.00 μm . Negative deviations in the marine particle size distribution give rise to large errors for $\lambda = 11.00 \mu\text{m}$. For 20% deviation, the error can be as high as 41%. The error decreases accordingly as the percent deviation is reduced.

TABLE OF CONTENTS

I.	INTRODUCTION	9
A.	MOTIVATION AND BACKGROUND	9
B.	ORGANIZATION	10
II.	THEORY	12
A.	EXTINCTION AND SCATTERING COEFFICIENTS	12
B.	ATMOSPHERIC AEROSOL MODELS	17
1.	Introduction	17
2.	Rural and Marine Aerosol Models	17
III.	PROCEDURE	21
A.	LOGIC	21
B.	CALCULATION OF OPTICAL DEPTH AND EXTINCTION COEFFICIENT	23
C.	ESTIMATION OF IR EXTINCTION COEFFICIENT	26
1.	Retrieval of TN and N ₂	27
2.	Calculation of β_{ext} at 3.75 and 11.00 μm	29
D.	VALIDITY OF NUMERICAL TECHNIQUES	29
IV.	RESULTS AND DISCUSSION	37
A.	BASIC RETRIEVAL ANALYSIS	37
B.	EXTINCTION ERROR ANALYSIS	38
C.	RELATIVE HUMIDITY ERROR ANALYSIS	39
D.	PARTICLE SIZE DISTRIBUTION ERROR ANALYSIS	42
E.	THREE-MODE PARTICLE SIZE DISTRIBUTION ERROR ANALYSIS	45
V.	CONCLUSIONS AND RECOMMENDATIONS	49
	LIST OF REFERENCES	51
	INITIAL DISTRIBUTION LIST	54

LIST OF TABLES

1. CHANGES IN AVERAGE MODE RADIUS (r_1 AND r_2) AS A FUNCTION OF RELATIVE HUMIDITY	18
2. BILINEAR INTERPOLATION VALIDITY TEST	32
3. ERROR ASSOCIATED WITH BASIC RETRIEVAL TECHNIQUE	38
4. ERROR ASSOCIATED WITH UNCERTAINTY IN EXTINCTION VALUE	40
5. RELATIVE HUMIDITY SENSITIVITY STUDY	45
6. PARTICLE SIZE DISTRIBUTION SENSITIVITY STUDY	47
7. EFFECT OF A THREE-MODE PARTICLE SIZE DISTRIBUTION	48

LIST OF FIGURES

2.1	Q_{ext} , particle distribution and β_{ext} for RH = 90% and $\lambda = 0.63 \mu\text{m}$ wavelength	14
2.2	Same as Fig. 2.1 but for $3.75 \mu\text{m}$ wavelength. Note change of scale for c	15
2.3	Variation of marine model size distribution of Shettle and Fenn (1979) with relative humidity	16
2.4	Three-mode Particle Size Distribution	20
3.1	Atmospheric Vertical Aerosol Distribution	22
3.2	Estimation of Extinction Coefficient at 3.75 from $0.63 \mu\text{m}$	24
3.3	Conversion of Digital Counts to Radiance	25
3.4	Outline of a Model for the Estimation of Extinction Coefficient	27
3.5	Bilinear Interpolation for Marine Case	30
3.6	Bilinear Interpolation for Rural Case	31
3.7	Monotonic Behavior of Mode 1 Radius for Marine and Rural models	33
3.8	Monotonic Behavior of Average Mode 2 Radius Size	34
3.9	Monotonic Behavior of Marine Scattering Coefficient	35
3.10	Monotonic Behavior of Rural Scattering Coefficient	36
4.1	Effect on the distribution of marine particles by changing RH by 20%	43
4.2	Effect on the distribution of rural particles by changing RH by 20%	44
4.3	Effect of Changing r_2 on the Distribution of Marine Particles	46

ACKNOWLEDGEMENTS

I thank Dr. Phil Durkee, my thesis advisor, for his long discussions and expert advice throughout the thesis study. Dr. Richard Franke of the Mathematics Department of the Naval Postgraduate School for his expert assistance and guidance in relation to the numerical techniques used throughout the course of this research project. Dr. C. Wash who carefully reviewed the manuscript and offered sound scientific and literary criticism. Finally, I thank my husband, Dale, whose encouragement and support have been invaluable to me during my graduate studies.

I. INTRODUCTION

A. MOTIVATION AND BACKGROUND

Electro-optical surveillance, guidance and weapon systems are affected by oceanographic and meteorological parameters (Mitchell *et al.*, 1982). Environmental features such as clouds, rain, relative humidity, haze, dust, aerosols and precipitation have been shown to have significant effects on the performance of these systems. Mitchell's study points out that systems such as the REWSON optical missile warning set used by helicopters, medium range air-to-surface missiles, the AEGIS combat weapon system (a fully automatic surface-to-air system) and high energy lasers have been found to be susceptible to the presence of aerosols in the atmosphere. These environmental parameters are not always considered in evaluating the performance of these weapon systems. This is because either the environmental information is not available, or the scale of the phenomena is so small that little confidence can be placed in the accuracy of its specification. In order to improve the evaluation of the performance of these systems the applicable parameters should be included for each weapon system.

Models such as the LOWTRAN 6 used for the evaluation of performance of certain missile systems can handle properly the absorption and scattering of radiation by water vapor for the prediction of transmission losses but improvement could be done in the initialization to account for a better representation of aerosols (Kneizys *et al.*, 1983). A joint effort by the Naval Research Laboratory, the Naval Postgraduate School and the Naval Ocean Systems Center is presently underway to develop a Navy Ocean Vertical Aerosol model (NOVAM) for inclusion into a future version of LOWTRAN. A different approach involving small modifications of LOWTRAN 6 could be done that would allow the insertion of an extinction coefficient value at the infrared wavelengths rather than the actual parameters needed to calculate the particle size distribution. This extinction coefficient value would be obtained from satellite estimates of optical depth and would take into account the aerosols present at the target location rather than at the point from where the weapon system is launched. This is important because some weapon systems rely on target signature in determining system performance. Target signature is related to the target-to-background

temperature difference, which, when propagated through the atmosphere, is modified by the transmittance and thus by the presence of aerosols.

Since there are weapon systems that operate at infrared, near-infrared and visible wavelengths, evaluation of the effect of environmental parameters must be performed at more than one wavelength. Estimating the extinction of the atmosphere (related to parameters such as visibility) must be done at the visible and near-infrared wavelengths and extrapolated to infrared wavelengths. This infrared extinction may be obtained from satellite measurements, but at the infrared wavelengths the power received from scattered radiation is small compared to visible wavelengths. Also, due to the presence of ambiguities from a variable background and water vapor, it is more practical to obtain measurements at visible wavelengths and estimate the extinction at the infrared wavelengths.

Studies by Gerber (1985) show that it is possible to use visible light scattered by aerosols to give useful estimates of extinction at infrared wavelengths. He showed that measurements using a combination of a two channel integrating nephelometer, which operates at one wavelength over two angular ranges, and an axial-scatter sensor gave the best accuracy ($\sim \pm 10\%$) for scaling over the 1.06-10.06 μm range for extinction by marine aerosols. However, his studies require direct measurement of the scattered light by the above instruments. The object of this thesis is to obtain an accurate representation of the size distribution of the aerosols in the marine atmospheric boundary layer from satellite measurements of radiance at visible wavelengths. The size distribution will then be used to obtain estimates of extinction coefficients at near-infrared and infrared wavelengths.

B. ORGANIZATION

The thesis is composed of five chapters. These include an introduction, theory, procedure, results and discussion, and a summary of conclusions and recommendations. Chapter II will discuss the theory of radiative scattering by atmospheric aerosols and the basic assumptions used in computing the scattering and extinction coefficients. A brief description of the atmospheric aerosol models is also included. Chapter III describes the model for estimating extinction coefficients at near-infrared and infrared wavelengths. It discusses the assumptions dealing with the vertical distribution of atmospheric particles in the marine boundary layer. Also included is the retrieval of the parameters required to describe the particle size

distribution of the aerosols and the calculation of extinction at 3.75 and 11.00 μm . Chapter III also discusses the validity of the numerical techniques used. Chapter IV discusses the procedure and results of five tests developed to evaluate the sensitivity and limitations of the models. A summary of the results and recommendations are stated in Chapter V.

II. THEORY

A. EXTINCTION AND SCATTERING COEFFICIENTS

Radiation can be scattered by air molecules, aerosol particles which are suspended in the air and by the earth's surface. Scattering by particles which are much smaller than the incident wavelength, such as molecules, is described by Rayleigh theory. Therefore, in the presence of gas molecules ($\sim 10^{-4}$ μm) and small particles (~ 0.05 μm), radiation undergoes Rayleigh scattering at visible wavelengths. For particles whose size are comparable to or larger than the wavelength, the scattering is referred to as Mie scattering. Thus, in the presence of cloud droplets (~ 10 μm) radiation undergoes Mie scattering at the infrared wavelengths, while in the presence of aerosols (~ 0.1 - 1.0 μm) radiation undergoes Mie scattering at the visible wavelengths. In a cloud-free environment away from large temperature or pressure gradients the molecular constituents do not vary in the horizontal appreciably and thus Rayleigh scattering does not vary significantly in the horizontal. However, Mie scattering depends on the size and number of aerosol particles. These particles are primarily generated by sea spray in a marine environment and are composed primarily of dust-like particles over the continents. Advection of these rural aerosols would result in large horizontal variations of the particle size distribution.

Scattering of light by aerosols is characterized by the extinction coefficient, β_{ext} . β_{ext} is given by the sum of the extinction by scattering and absorption.

$$\beta_{\text{ext}} = \beta_{\text{scat}} + \beta_{\text{abs}} \quad (2.1)$$

Absorption of radiation by aerosols is described by the complex part of the index of refraction. For marine particles the complex part of the index of refraction is less than 10^{-4} at wavelengths less than 1 μm , and therefore absorption by marine aerosols is very small (Shettle and Fenn, 1979). For visible and near infrared wavelengths, β_{ext} for marine aerosols is approximately equal to β_{scat} . For higher wavelengths and for rural cases, the complex part of the index of refraction is of order 10^{-2} so both terms must be included in the calculation of extinction at 3.75 and 11.00 μm . Gases in the atmosphere, such as CO_2 and water vapor, absorb radiation. However, at the

wavelengths of interest (0.63, 0.86, 3.75 and 11.00 μm) the absorption by these constituents is small and can be neglected in our calculations.

Given the size and distribution of these particles, the extinction coefficient (in units of per length) is defined as:

$$\beta_{\text{ext}} = \int_0^{\infty} \pi r^2 Q_{\text{ext}}(m, r) (dN(r)/dr) dr, \quad (2.2)$$

where Q_{ext} is the extinction efficiency of a particle with radius r and complex index of refraction m , and dN/dr describes the size distribution of the particles. As seen in Eqn. 2.2, the extinction coefficient depends on three terms: the cross-sectional area (πr^2), the extinction efficiency (Q_{ext}) and the size distribution (dN/dr). The relationship of r , Q_{ext} and dN/dr for a typical visual case is presented in Fig. 2.1. Panel b of Fig. 2.1 shows a particle size distribution for a relative humidity (RH) value of 90% composed of two modes. The modes correspond to small (mode 1) and large (mode 2) radii particles. The nature of each mode is described in detail in II. B. This example shows that when r is small, πr^2 and Q_{ext} are small, while dN/dr is large; when r is large, πr^2 is large and dN/dr and Q_{ext} become small. The result is that β_{ext} is affected by a bounded region of particle sizes. Low values of Q_{ext} bound β_{ext} at the small radii while a decrease in dN/dr bounds β_{ext} at the large radii. For visible wavelengths and a marine aerosol size distribution model at 80% relative humidity, studies done by Durkee (1987) include a particle range from approximately 0.5 to 5.0 μm . To account for variations in wavelength and relative humidity this study incorporates a radii range from 0.01 to 50.0 μm in the extinction coefficient calculation.

The extinction efficiency function is dependent on wavelength and relative humidity since composition changes with increased condensed water. As wavelength increases Q_{ext} shifts to the right, weighing larger radius particles more than smaller particles as depicted by Figs. 2.1 and 2.2. Since there are fewer particles at the larger radii the net effect of increasing wavelength is a decrease in the extinction coefficient, β_{ext} . Fig. 2.3 shows the effect of relative humidity on the size distribution of marine particles. Notice the increase in the number of large particles for higher relative humidity values on Fig. 2.3. Since the Q_{ext} function at 3.75 μm weighs the larger particles (greater than the mode radius) more than smaller particles, and there are more particles at the larger radii, the net effect is an increase in the cumulative extinction for higher relative humidity values.

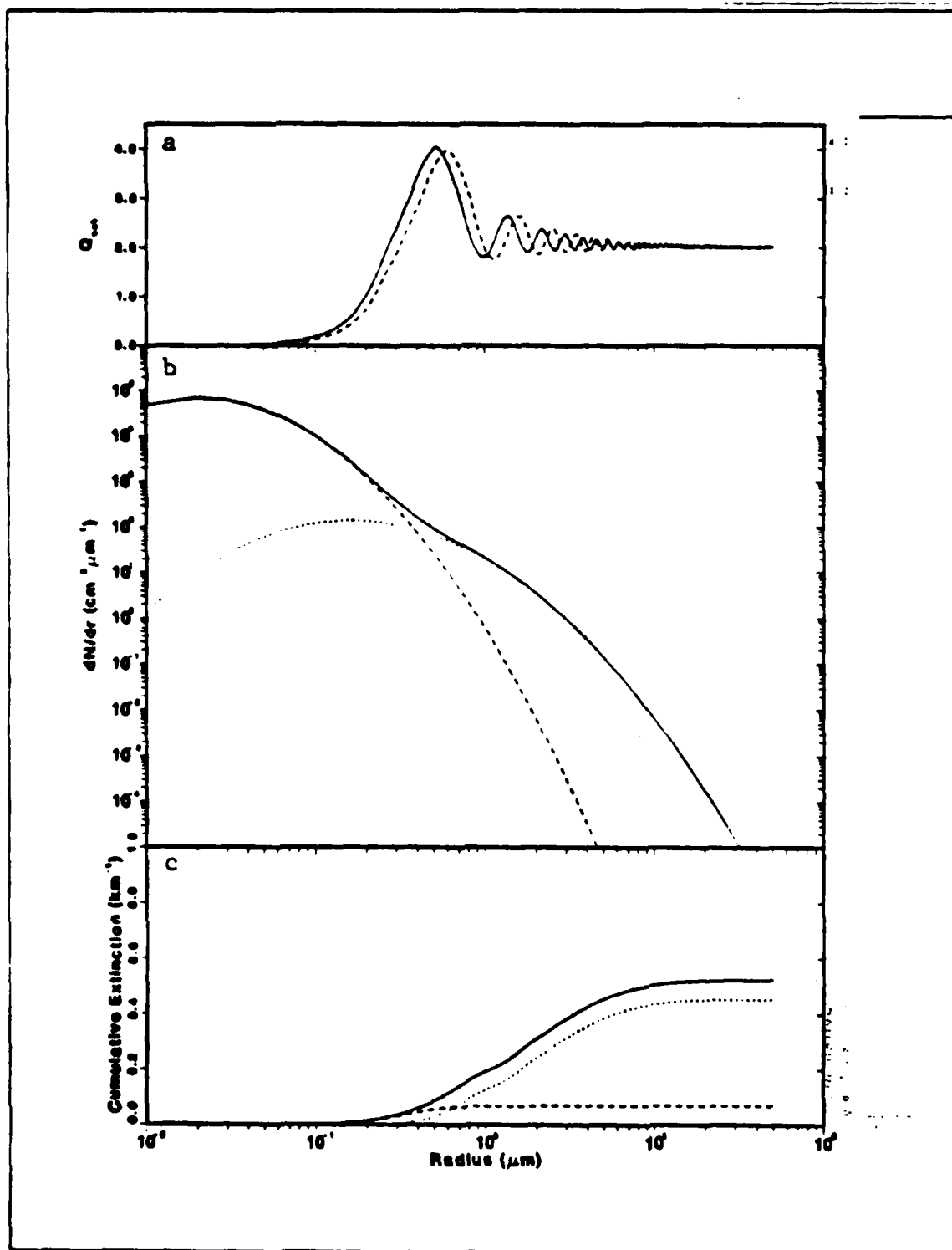


Fig. 2.1 a. Extinction efficiency for $\lambda = 0.63 \mu\text{m}$ and RH = 90% for mode 1 (solid) and mode 2 (dashed). b. Model distribution of marine particles at RH = 90%. Sum mode 1 & 2 (solid), mode 1 (dashed), mode 2 (dot). c. Cumulative extinction from Eqn. 2.2.

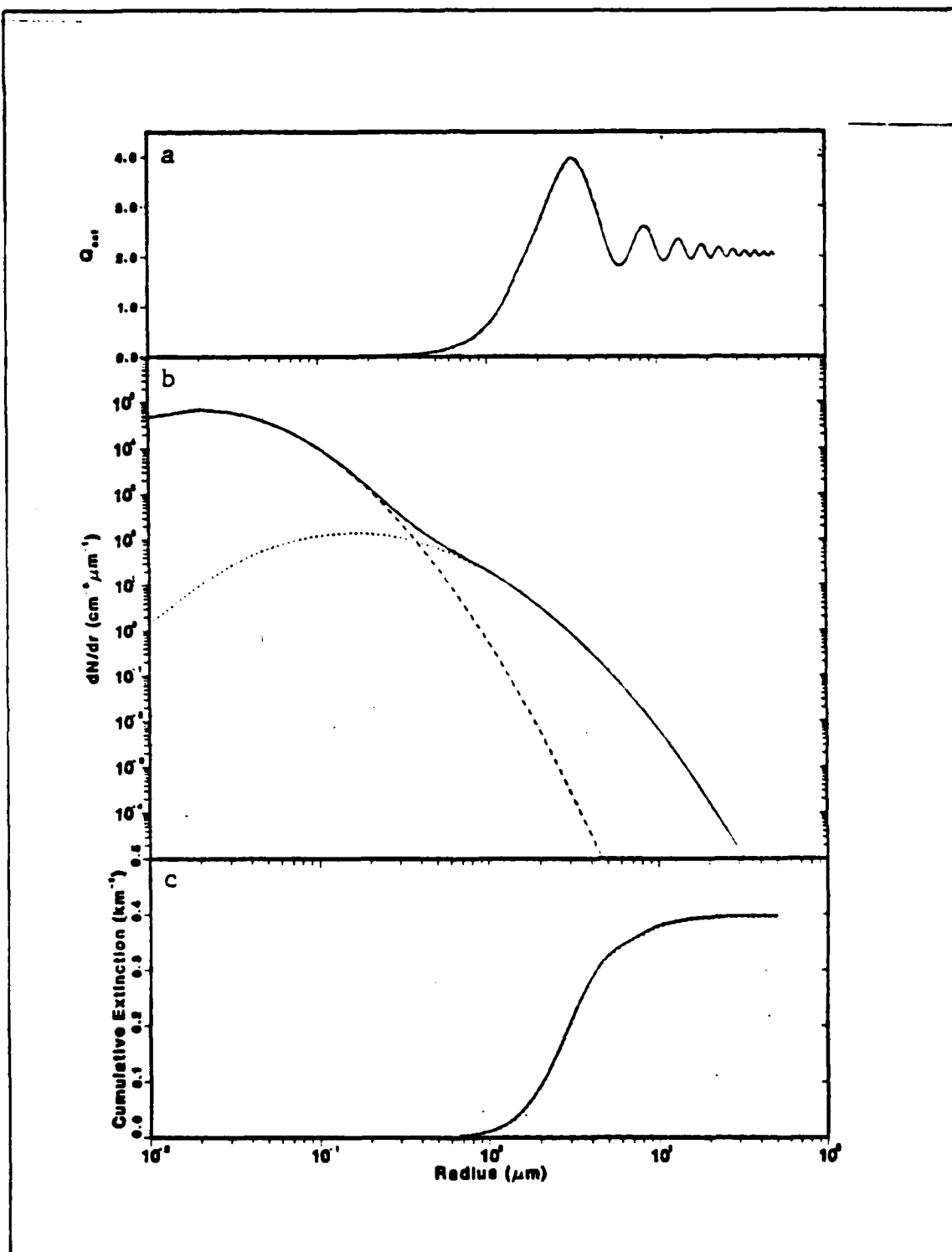


Fig. 2.2 Same as Figure 2.1 but for $3.75 \mu\text{m}$ wavelength. Note change of scale for c.

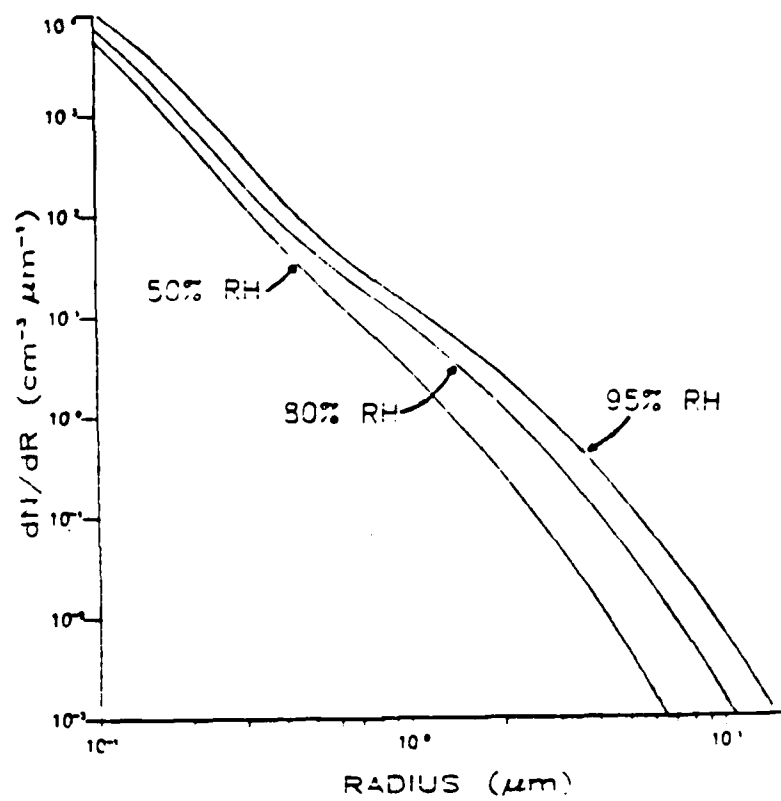


Fig. 2.3 Variation of marine model size distribution of Shettle and Fenn (1979) with relative humidity.

B. ATMOSPHERIC AEROSOL MODELS

1. Introduction

Atmospheric aerosol particles in the atmosphere vary greatly in their concentration, size and composition, and consequently in their effects on optical and infrared radiation. Several tropospheric aerosol models have been developed by Shettle and Fenn (1979) which include the dependence of atmospheric aerosols on relative humidity.

The size distribution for the different aerosol models used here are represented by the sum of two log-normal distributions:

$$\frac{dN}{dr} = \sum_{i=1}^2 \left(\frac{N_i}{\ln(10) r \sigma_i \sqrt{2\pi}} \right) \exp \left[- \frac{(\log r - \log r_i)^2}{2 \sigma_i^2} \right] \quad (2.3)$$

where N is the cumulative number density of particles of radius r ; σ is the standard deviation; r_i , N_i are the mode radius and the total number density. This form of the distribution function represents the multimodal nature of the atmospheric aerosols which will be discussed next. This study will begin with a bimodal size distribution since it has been shown to be generally adequate to characterize the gross features of most aerosol distributions (Whitby and Cantrell, 1975). A third mode will be added to allow for wind generated, larger than 2 μm mode radii, particles. The rural model is comprised of a small rural aerosol mode (mode 1) and a large rural aerosol mode (mode 2). The marine model consists of a small rural aerosol mode (mode 1) and an oceanic mode (mode 2).

2. Rural and Marine Aerosol Models

The rural model is intended to represent the aerosol under conditions where it is not directly influenced by urban and/or industrial aerosol sources. The aerosols are assumed to be composed of a mixture of 70 percent of water soluble substance and 30 percent dust-like aerosols. The marine aerosol model is composed of a sea-salt mode and a continental mode which was assumed to be identical to the rural aerosol with the exception that the very large particles were eliminated since they will be eventually lost due to fallout as the air masses move across the oceans. The relative proportions of aerosols of oceanic or continental origins will vary, particularly in coastal regions. To

account for these variations, the model permits adjustment of the relative contribution by the oceanic and continental modes. The contribution from the marine size distribution used in this study varied from zero to 6% of the total number of particles of oceanic origin while the large rural aerosols varied from zero to 0.025%. The small radii particles, mode 1, make up the rest and were changed accordingly.

As relative humidity increases, water vapor condenses out of the atmosphere onto the particulates suspended in the atmosphere. This condensed water increases the size of the aerosols and changes their composition and their effective refractive index. The resulting effect of the aerosols on the absorption and scattering of light will be modified correspondingly. Table 1 shows how the size of a particle changes with relative humidity for both the rural and oceanic models. As relative humidity increases, the mode radii increases for all modes and thus the number of particles at a given radius increase with the larger radii increasing the most, as seen previously in Fig. 2.3.

TABLE 1
CHANGES IN AVERAGE MODE RADIUS (r_1 AND r_2) AS A
FUNCTION OF RELATIVE HUMIDITY

RELATIVE HUMIDITY	RURAL		MARINE r_2 (μm)
	r_1 (μm)	r_2 (μm)	
0%	0.02700	0.4300	0.1600
50%	0.02748	0.4377	0.1711
70%	0.02846	0.4571	0.2041
80%	0.03274	0.5477	0.3180
90%	0.03884	0.6462	0.3803
95%	0.04238	0.7078	0.4606
98%	0.04751	0.9728	0.6024
99%	0.05215	1.7555	0.7505

The marine model was modified to allow the addition of a wind driven third mode to the size distribution. As shown in Fig. 2.4 this third class of aerosol consists

of the largest nuclei originating from the sea surface. It has a mode radius of 2 μm and the amplitude varies with wind speed (Gathman, 1983). These large particles can be important in the propagation of infrared radiation near the sea surface under a condition of high winds.

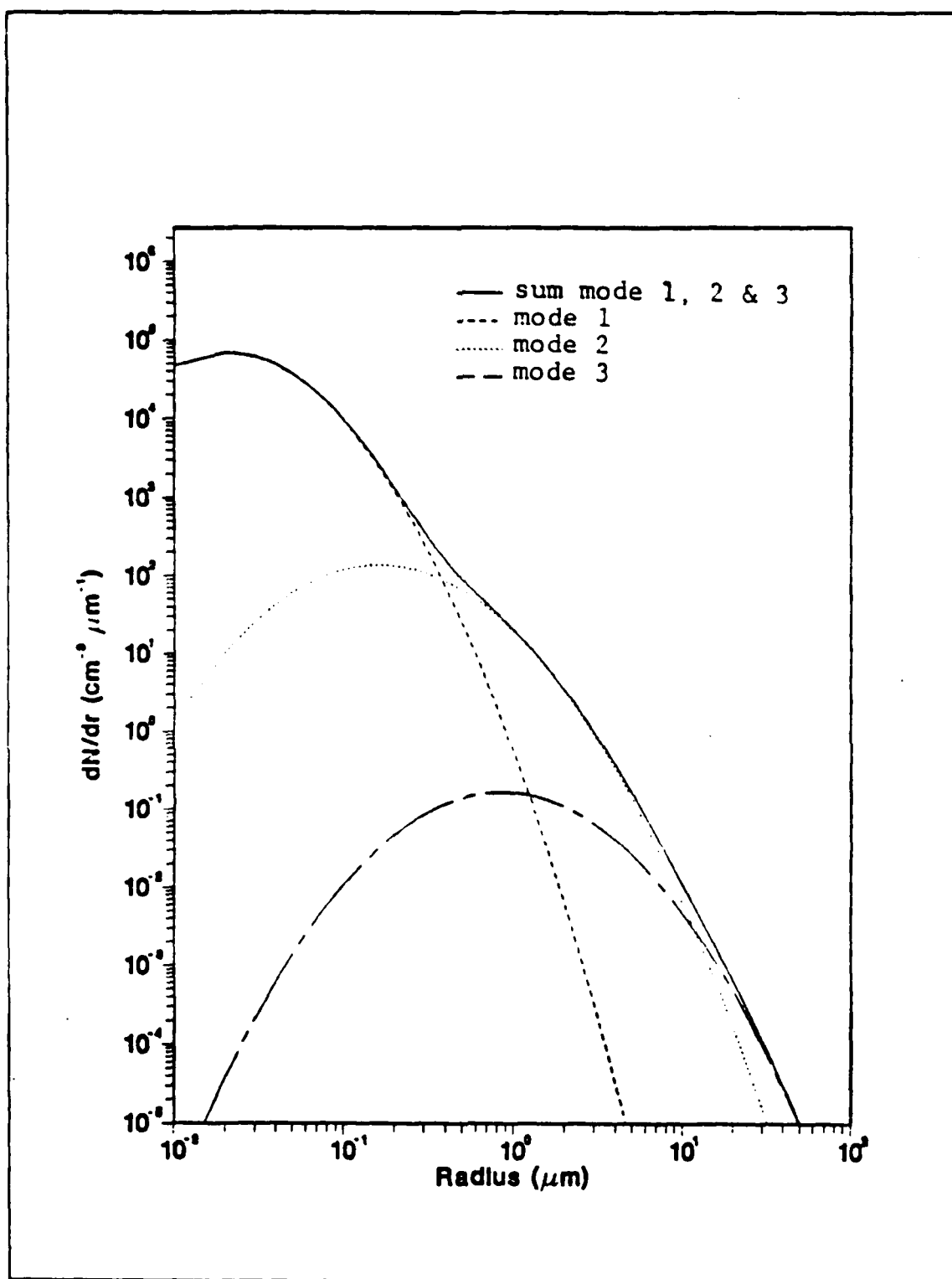


Fig. 2.4 Three-mode particle size distribution for marine model at RH = 90% and A3 = 1.0. Sum of modes 1 & 2 (solid), mode 1 (dashed), mode 2 (dot), mode 3 (chain-dash).

III. PROCEDURE

A. LOGIC

The main goal of this study is to be able to estimate extinction coefficients at near-infrared and infrared wavelengths from satellite information at shorter wavelengths. Channel 1 (0.55 to .68 μm) and channel 2 (0.70 to 1.00 μm) of the NOAA-7 Advanced Very High Resolution Radiometer (AVHRR) return image information from which a value of radiance is obtained. Since radiance can be shown to be a nearly linear function of aerosol optical depth (Durkee *et al.*, 1986), the optical depth due to the presence of aerosols can be calculated as discussed in III. B.

The optical depth is calculated from integration of the extinction coefficient:

$$\tau = \int \beta_{\text{ext}} dz \quad (3.1)$$

Above the boundary layer, as shown in Fig. 3.1 (Fairall and Davidson, 1986), the volume of aerosols decreases due to a decline in relative humidity, and therefore the extinction coefficient, will decrease as discussed in Chapter II. A. Thus, the extinction above the top of the marine atmospheric boundary layer (MABL) can be considered negligible since the number of particles above this height is significantly reduced. The integration is thus simplified and β_{ext} can be approximated from:

$$\beta_{\text{ext}} = \tau/Z, \quad (3.2)$$

where Z is the height of the top of the MABL. Therefore, β_{ext} can be estimated from satellite estimates of τ and estimates of Z obtained from models such as the Fleet Numerical Oceanography Center's Navy Operational Local Analysis and Prediction System (NOLAPS) (Burk and Thompson, 1982). Later in this chapter it will be shown that this extinction value is the input required in the model in order to retrieve a particle size distribution which is used to calculate the extinction at other wavelengths.

A simple technique for estimating extinction coefficient at longer wavelengths was attempted by plotting extinction coefficient values in the visible and near-infrared. Fig. 3.2 shows the relationship between extinction coefficients at 0.63 and 3.75 μm for

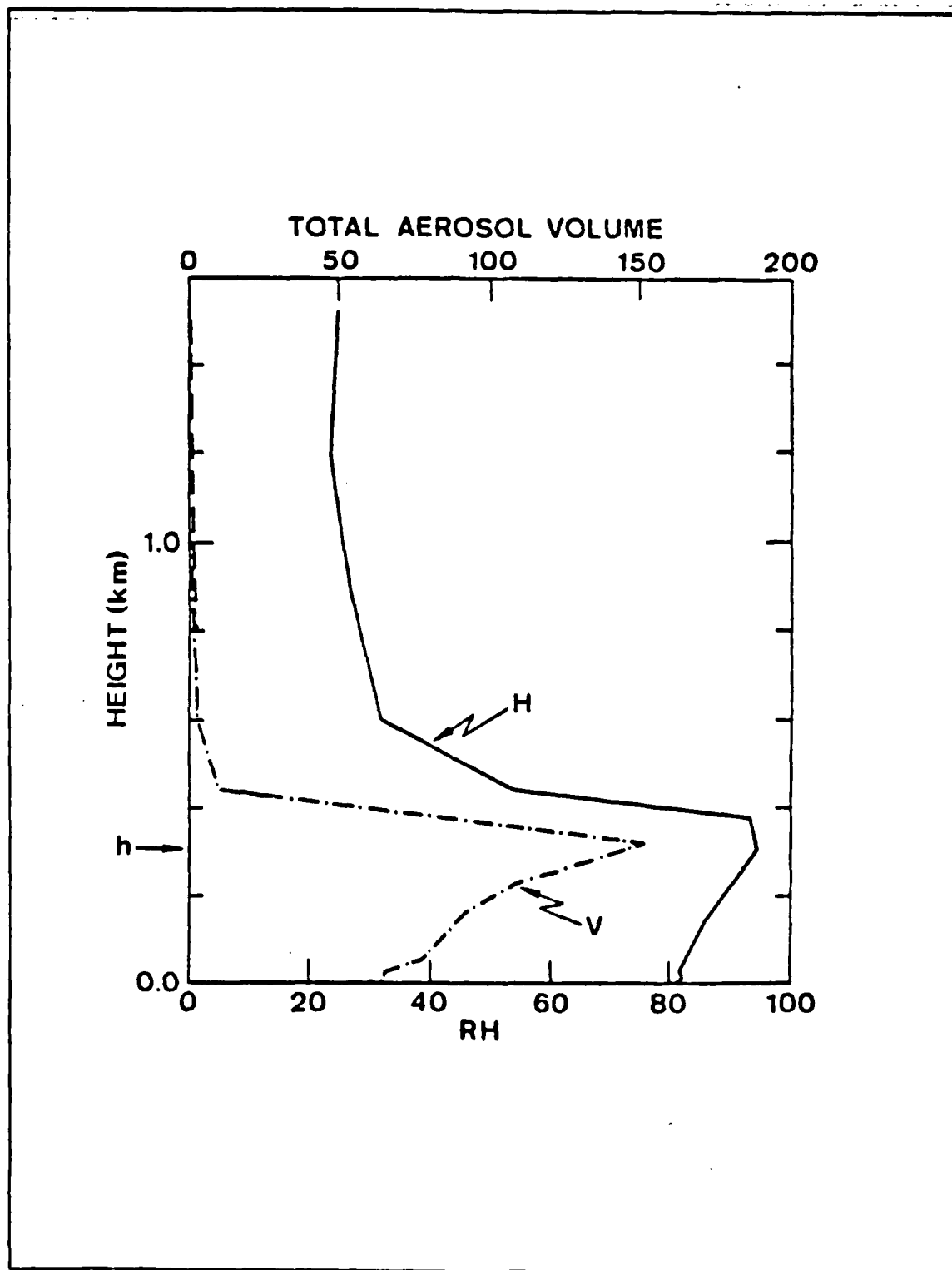


Fig. 3.1 Height dependence of aerosol volume (V) and RH (H) above the ocean shows a decrease in aerosol above MABL due to a decrease in RH. (Fairall and Davidson, 1986).

three values of the contribution of the second mode, N2. Each distribution case is varied by changing relative humidity. The total number of particles, TN, was set at $4,000 \text{ cm}^{-3}$, relative humidity, RH, varied from 0 to 99%, and the contribution of the second mode, N2, was set at 0.0, 0.000125 and 0.000250 for each line respectively. In order to find extinction values at 3.75 and 11.00 μm an infinite number of plots similar to Fig. 3.2 would have to be generated, one for each distribution shape. A simple prediction using one wavelength is therefore impossible. This result is consistent with Gerber (1985) who showed for various atmospheric simulations that no correlation exists between extinction at visible and near-infra red wavelengths when scaling with only one wavelength.

We have shown that the extinction value depends on the number of particles present and on their distribution. Thus, a method using satellite-detected radiance at two wavelengths is proposed for estimating extinction at the 3.75 and 11.00 μm wavelengths. Approximations made in order to convert radiance measurements from satellite data to an extinction value are discussed in III. B. From an input of extinction values at 0.63 and 0.86 μm the model can retrieve the total number of particles (TN) and the percentage of the second mode (N2). With knowledge of these parameters, which are needed to describe the particle size distribution, and an effective humidity value for the boundary layer, the model can calculate extinction at 3.75 and 11.00 μm as discussed in III. C.

B. CALCULATION OF OPTICAL DEPTH AND EXTINCTION COEFFICIENT

Channel 1 (0.63 μm) and channel 2 (0.86 μm) of the NOAA-7 AVHRR satellite returns image information in the form of digital brightness counts. A digital number (which is proportional to the amount of radiation received at a satellite) is assigned to each image element. This inserts some uncertainty since only integers are used in the digitizing process. Fig. 3.3 shows the conversion between digital counts and physical units for the AVHRR (Durkee, 1984).

The radiance at satellite altitude (L_S) consists of contributions from the following terms:

$$L_S = (L_W + L_G)T + L_R + L_A . \quad (3.3)$$

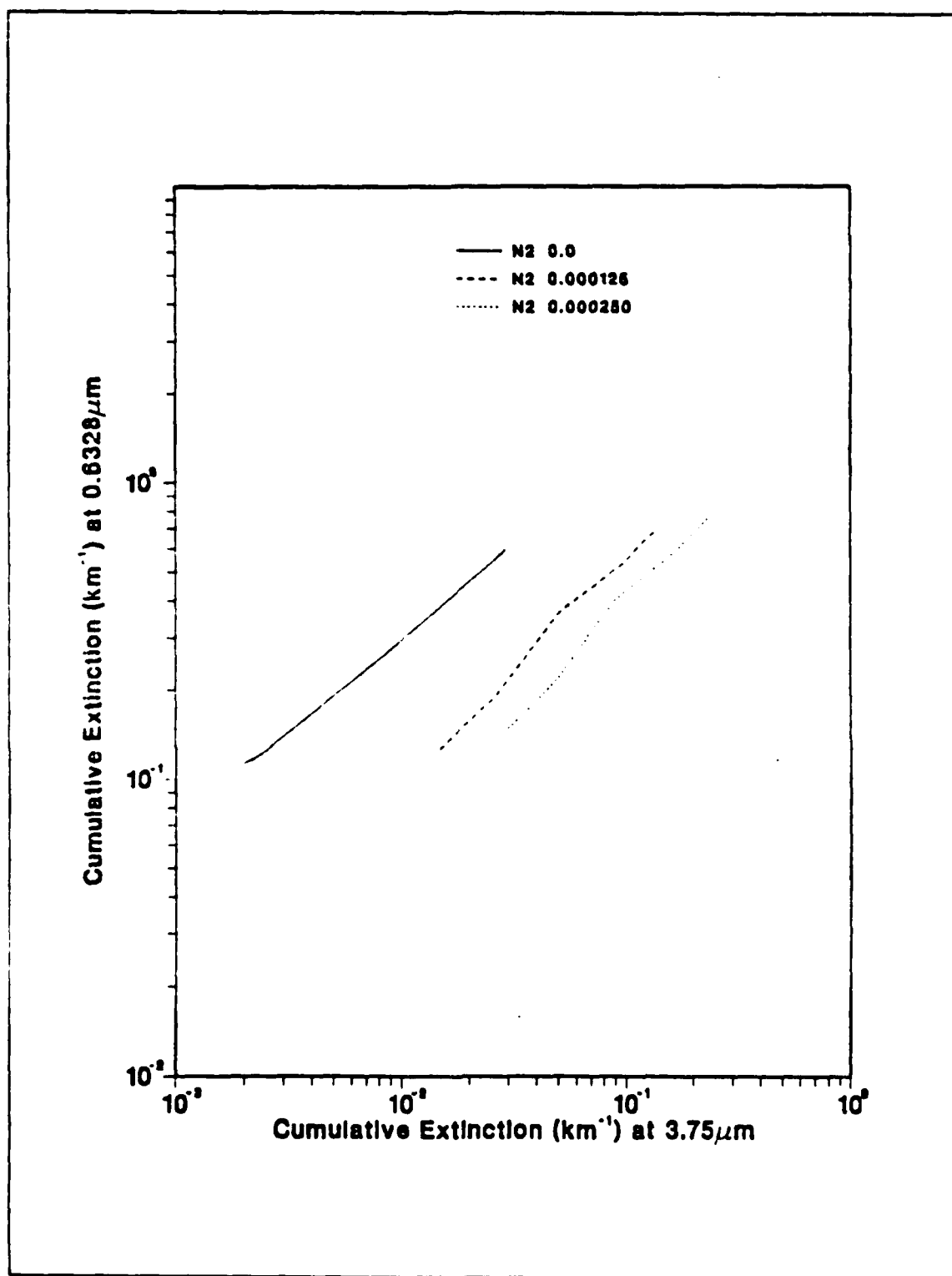


Fig. 3.2 Estimation of extinction coefficient at 3.75 μm from 0.63 μm for three different particle size distribution, described by N2.

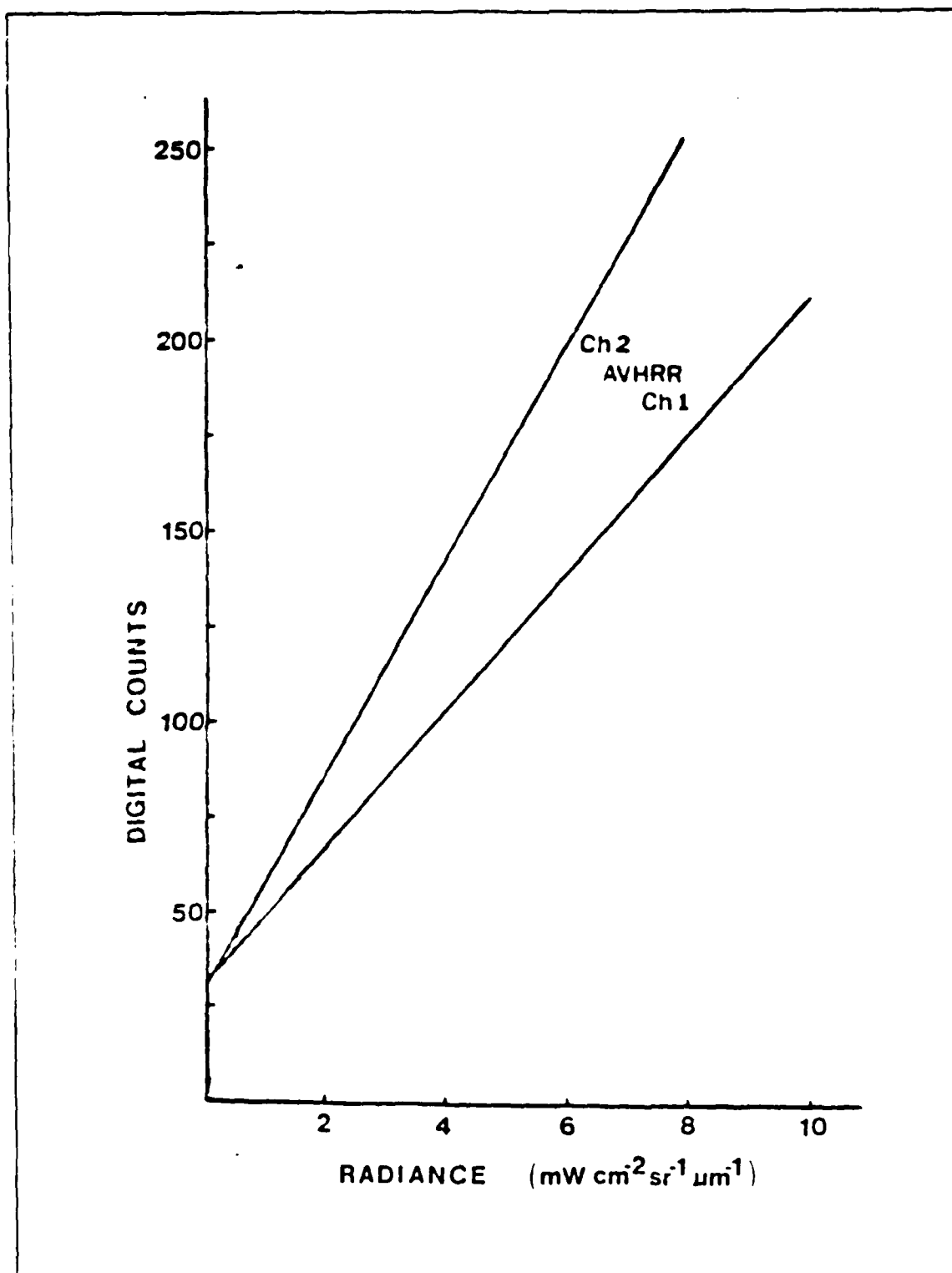


Fig. 3.3 Conversion of digital counts to radiance for the AVHRR sensors (Durkee, 1984).

where L_W is the 'water leaving' radiance caused by subsurface reflectance, L_G is the contribution from the specular reflection off the sea surface, L_R is the path-added radiance due to Rayleigh scattering in the atmosphere, L_A is the path-added radiance due to Mie scattering in the marine boundary layer and T is the atmospheric transmittance.

For wavelengths in the red-visible to near-infrared, L_W generally will be a small contribution to upwelling radiance. L_G , also referred to as the radiance added by 'sunglint', can be estimated from knowledge of the sun-earth-satellite geometry and surface roughness. L_G is negligible under all but certain geometries. L_R is obtained from knowledge of the Rayleigh optical depth (which can be estimated from profiles of pressure and temperature) and scene geometry (McCartney, 1976).

In the single scattering approximation we consider the radiation which is scattered only once by marine aerosols. If we assume that the upward intensity at the bottom of the atmosphere is zero and for atmospheres with small optical depth, it can be shown that radiance is a linear function of optical depth (Durkee *et al.*, 1986). The optical depth due to the presence of aerosols can then be estimated from the aerosol radiance. Eqn. 3.2 can then be used to calculate the extinction coefficient required for input into the model. For the purpose of this study it is assumed that the extinction values at 0.63 and 0.86 μm are available from estimates of optical depth (τ) and boundary layer depth (Z).

C. ESTIMATION OF IR EXTINCTION COEFFICIENT

Fig. 3.4 shows a basic outline of the model for estimating extinction at near-infrared and infrared wavelengths. This model can be divided into two sections. In the first part of the model, input of the aerosol model type (marine or rural) and the effective relative humidity for the MABL defines the location of the average mode radius, r_1 and r_2 . Input of the extinction coefficient at 0.63 and 0.86 μm will determine the magnitude of the retrieved total number of particles, TN , and percentage distribution of the second mode, N_2 . These are the parameters necessary to describe the distribution of the aerosols particles. The second part of the model uses these values of TN and N_2 and an effective relative humidity value for the boundary layer to estimate the extinction coefficient at 3.75 and 11.00 μm .

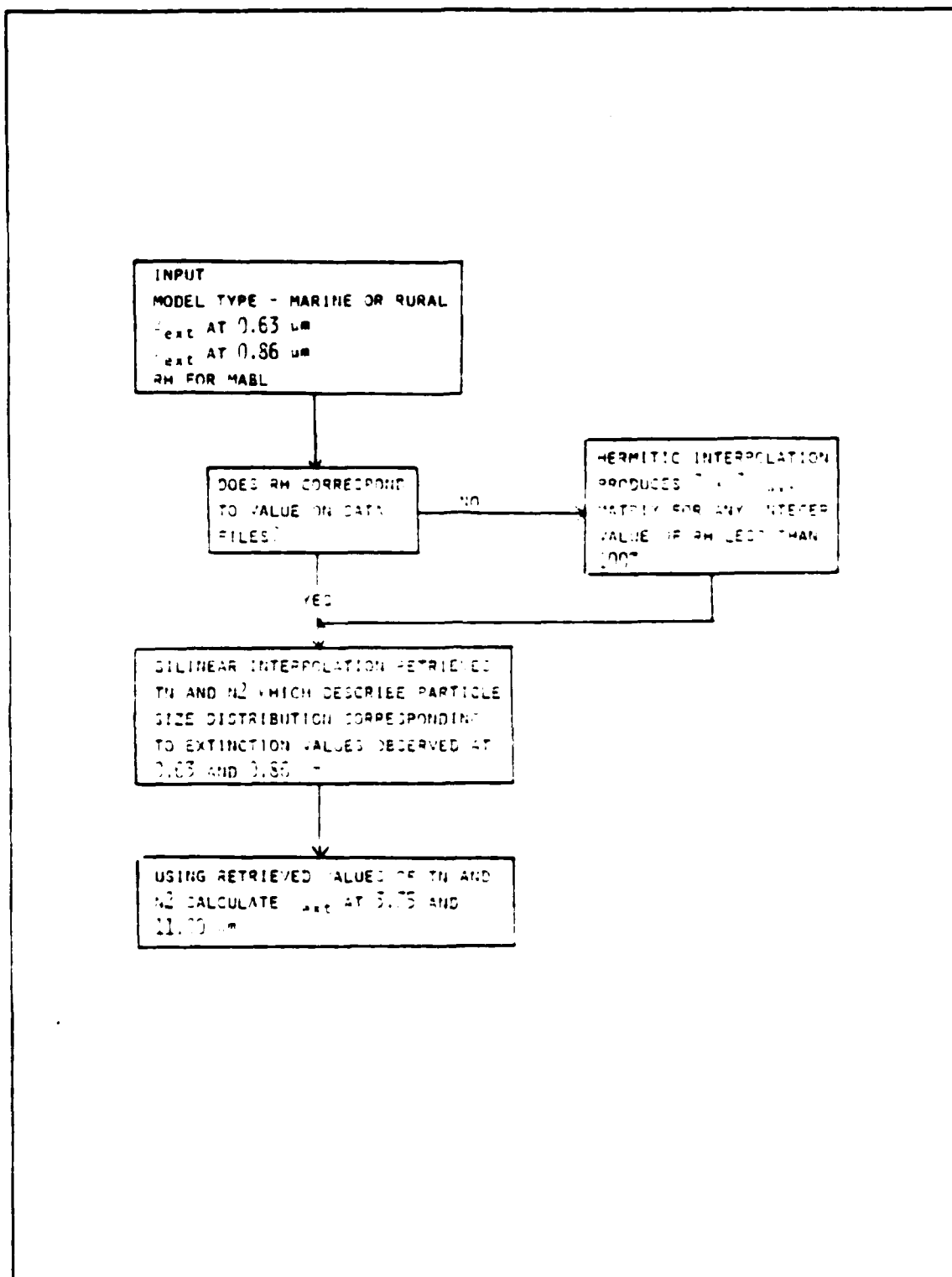


Fig. 3.4 Outline for the estimation of extinction coefficients at NIR and IR wavelengths.

1. Retrieval of TN and N2

This portion of the model is used to calculate the total number of particles and the contribution of the second mode needed to describe the aerosol distribution using a bilinear interpolation. The model's application is limited by the total number of particles and the variations allowed. For this study, in the marine case, TN was allowed to vary from 1,000 to 7,000 cm^{-3} and the second mode contribution, N2, varied from 0.0 to 0.06. For the rural case, TN was allowed to vary from 10,000 to 20,000 cm^{-3} and the second mode contribution, N2, varied from 0.0 to 0.000250. These are the current limitations of the model but the model can be easily expanded to allow for greater variations. The data files are comprised of 7 X 7 β_{ext} matrices for marine and rural cases at 0.63 and 0.86 μm , and for RH = 0, 50, 70, 80, 90, 95, 98 and 99%. These matrices were obtained by running the second portion of the model for the following values of TN and N2. For the marine case, N2 values used were 0.0, 0.01, 0.02, 0.03, 0.04, 0.05 and 0.06. For the rural case N2 values used were 0.0, 0.000050, 0.000100, 0.000125, 0.000150, 0.000200, 0.000250. In order to run the model, an effective humidity for the boundary layer and values of extinction at 0.63 and 0.86 μm must be entered. A subroutine in the model, using a Hermite interpolation, allows calculation of a 7 X 7 β_{ext} matrix for any integer value of relative humidity less than 100% not in the data files.

As discussed in II. A., β_{ext} is a function of TN, N2, RH and λ . An infinite number of combinations of TN and N2 will give rise to a predetermined extinction coefficient at a given wavelength. But only one TN and N2 combination will give rise to a given β_{ext} at λ_1 and a given β_{ext} at λ_2 . Therefore, we must generate lines describing these combinations at each wavelength and solve for the intersection of these two lines which will give the value of TN and N2 associated with the input β_{ext} at the two visible wavelengths.

The following description shows how the model mathematically solves for the two parameters, TN and N2, needed to describe the aerosol distribution in question. For a given extinction value, a corresponding TN value is calculated at each N2. This generates a set of seven values of TN, one at each N2 value, for each λ . The intersection between the curves formed by these sets (Figs. 3.5 and 3.6) represents the best approximation of TN and N2 which describes the particle distribution corresponding to the extinction coefficient value observed at 0.63 and 0.86 μm . This single value of TN and N2 is obtained by a bilinear interpolation. The bilinear

interpolation consists of obtaining an equation for each line using a point-form for the nearest point on each side of the intersection. By solving the two equations the intersection of the two curves is determined and therefore an estimate of TN and N2 is obtained.

2. Calculation of β_{ext} at 3.75 and 11.00 μm

This portion of the model calculates an extinction coefficient value, β_{ext} , at near-infrared and infrared wavelengths, from knowledge of the particle size distribution and an effective value of relative humidity for the marine boundary layer. Data files containing mode radii for marine and rural cases are supplied. These values have been interpolated using a Hermite interpolation for integer values of relative humidity ranging from 0 to 99%. Also included are data files containing values of index of refraction for marine and rural cases. These values have also been interpolated using a Hermite interpolation for integer values of relative humidity ranging from 0 to 99%. Uninterpolated values for mode radii and index of refraction at RH = 0, 50, 70, 80, 90, 95, 96, 97, 98 and 99% were obtained from Shettle and Fenn (1979). The value of TN and N2 obtained from the previous portion of the model and an effective relative humidity, RH, for the marine boundary layer are entered into the model. Using Eqns. 2.3 and 2.2 the model calculates β_{ext} at 3.75 and 11.00 μm .

D. VALIDITY OF NUMERICAL TECHNIQUES

Values for the average radius of each mode, r_1 and r_2 , and the real and imaginary parts of the index of refraction for the marine and rural cases are provided for only certain relative humidity values as discussed in the previous section. Figs. 3.7 and 3.8 are a plot of the average mode radius as a function of relative humidity and show a monotonic behavior for both r_1 and r_2 . Due to the flat section followed by a rapid nonlinear portion for relative humidity values greater than 70%, a Hermite cubic numerical interpolation was used to generate values of r_1 and r_2 for relative humidity values ranging from 0 to 99%. Figures 3.9 and 3.10 show a similar monotonic trend for the scattering extinction for rural and marine cases as a function of relative humidity. Based on this result, matrices needed for extinction values during the retrieval portion of the model are generated by a Hermitic interpolation. The real and imaginary portions of the index of refraction also follow this behavior and a Hermitic interpolation was therefore employed. The Hermitic cubic function in this program was developed by the Lawrence Livermore National Laboratory (Fritsch, 1982). Such

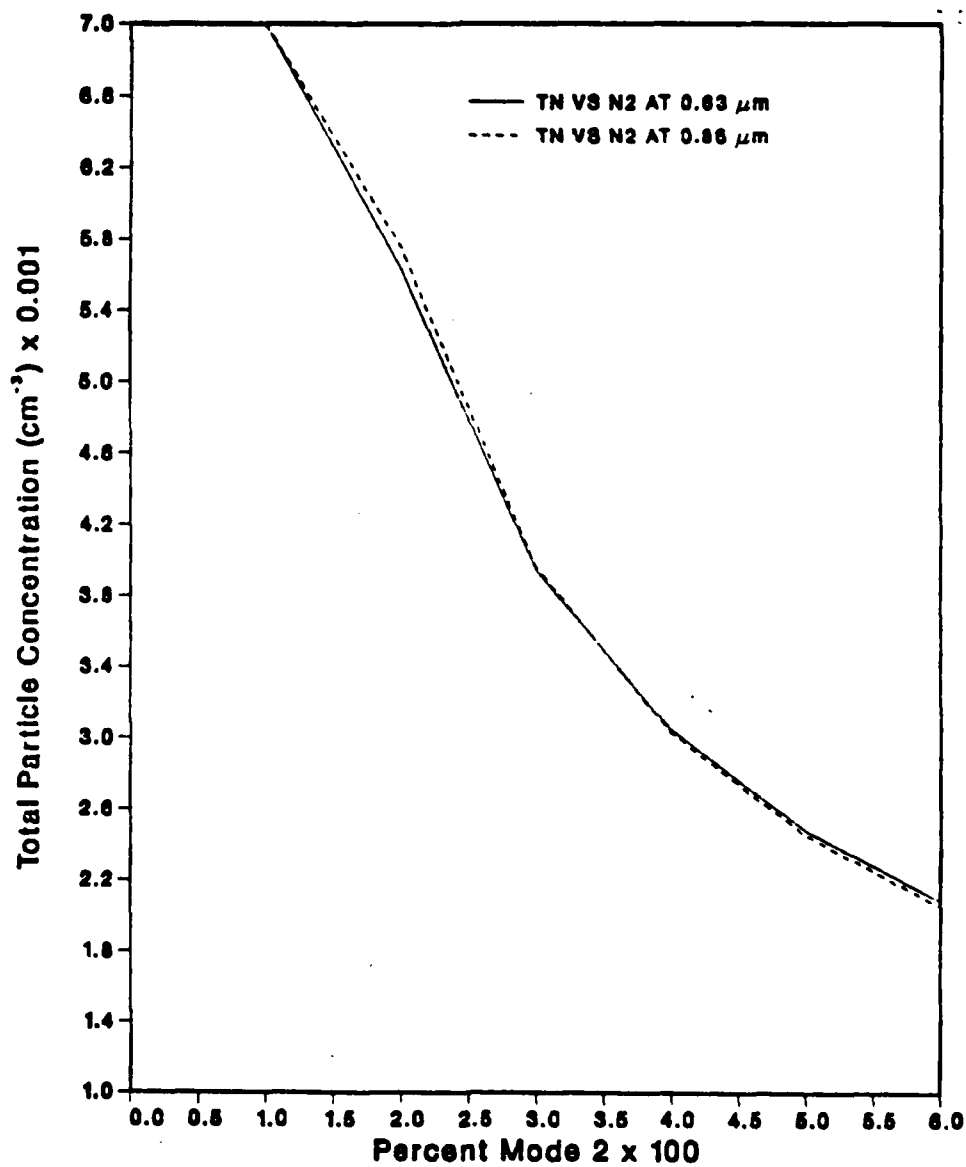


Fig. 3.5 TN value for corresponding N2 at 0.63 (solid) and 0.86 (dashed) μm wavelength. Intersection gives best estimate of TN and N2 for aerosol marine distribution given by input extinction coefficients.

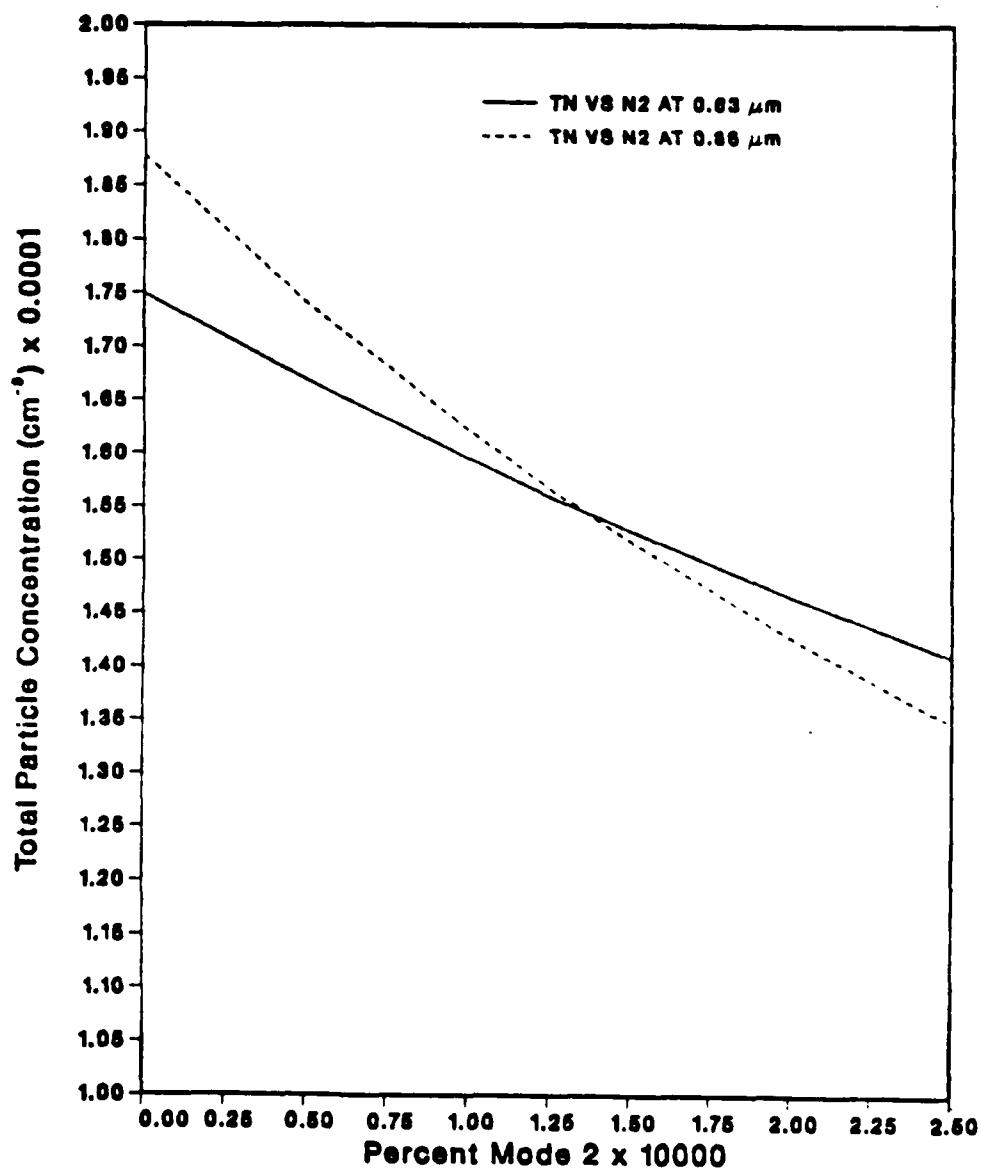


Fig. 3.6 TN value for corresponding N2 at 0.63 (solid) and 0.86 (dashed) μm wavelength. Intersection gives best estimate of TN and N2 for the rural aerosol distribution given by input extinction coefficients.

an interpolating scheme is more reasonable than a cubic spline if the data contain both "steep" and "flat" sections as shown in Figs. 3.7 - 3.10.

As discussed in the previous section, a bilinear interpolation was used to solve for the intersection of the two lines and retrieve the parameters, TN and N2, needed to describe the particle size distribution of aerosols. This technique was appropriate for this case, as seen in Figs. 3.5 and 3.6, since the equation of the lines are generated with points in the immediate vicinity of the intersection and a linear approximation between such short distances can be made. Fig. 3.5 shows that if the points were separated a greater distance a linear approximation would not hold true for the marine case since over the interval used for N2 (0.0 to 0.06) the curve is not linear. However, it would still hold true for the rural case since the lines are almost linear as seen in Fig. 3.6. For the rural case the values immediately following the intersection (A1-A4) were used to find the intersection point. A set of values (B1-B4) further away from the intersection were used and compared with the first set. Prediction errors for extinction at 3.75 and 11.00 μm were calculated. The results shown in Table 2 show excellent agreement since the errors are less than 1% for both infrared wavelengths. Thus the bilinear interpolation is suitable for the rural case and in this study an acceptable method of interpolation for the marine case.

TABLE 2
BILINEAR INTERPOLATION VALIDITY TEST

INPUT		$\beta_{\text{ext}}(\text{km}^{-1})$		ERROR(%)	
		3.75 μm	11.00 μm	3.75 μm	11.00 μm
	TN 15575 cm^{-3}	0.02446	0.01595	--	--
	N2 0.000115				
A	TN 15551 cm^{-3}	0.02443	0.01593	-0.12	-0.12
	N2 0.000114				
B	TN 15550 cm^{-3}	0.02443	0.01593	-0.12	-0.12
	N2 0.000112				

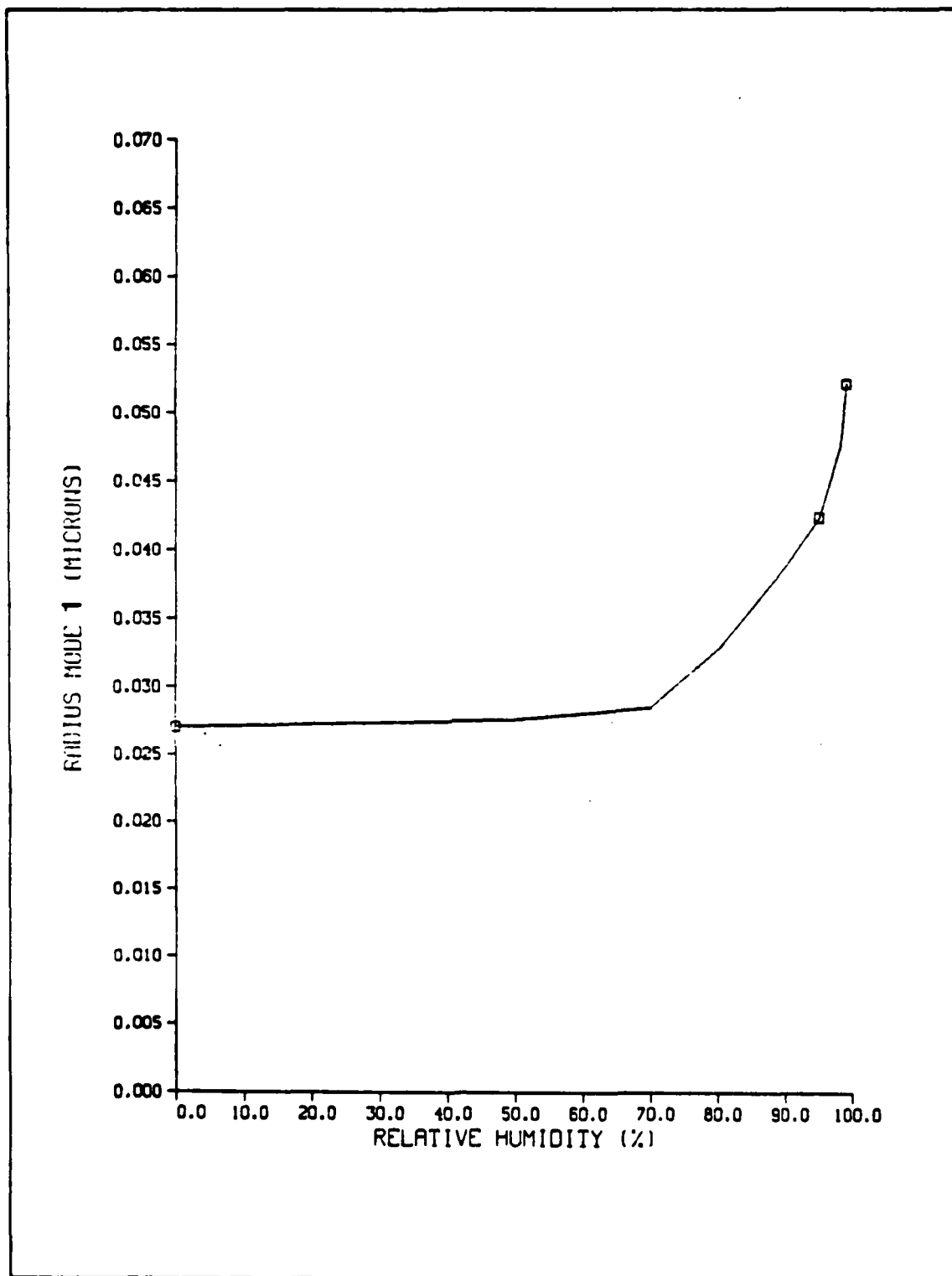


Fig. 3.7. Monotonic behavior of the average mode 1 radius for marine and rural models from Table I.

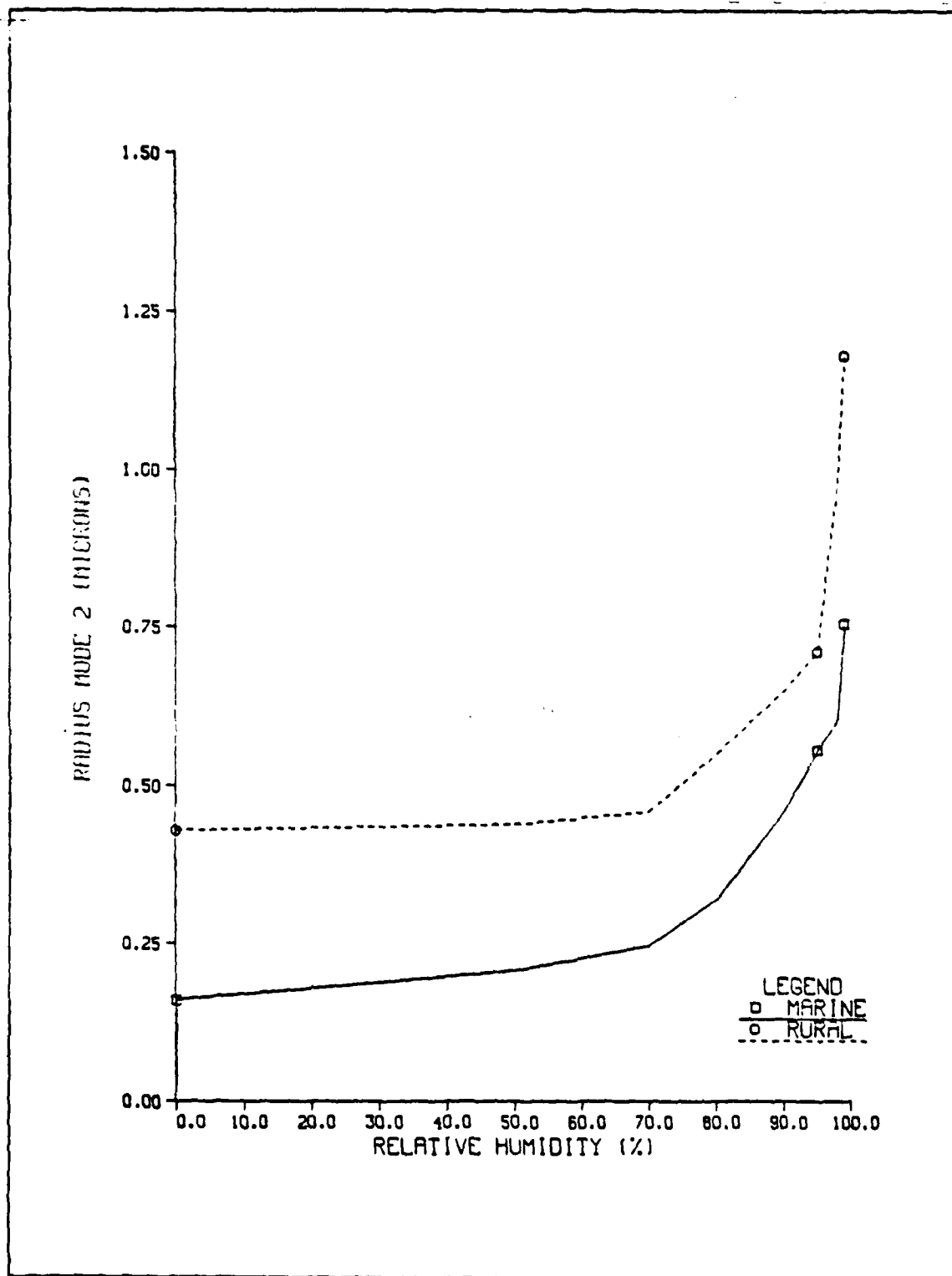


Fig. 3.8 Monotonic behavior of the average mode 2 radius for marine and rural models from Table I.

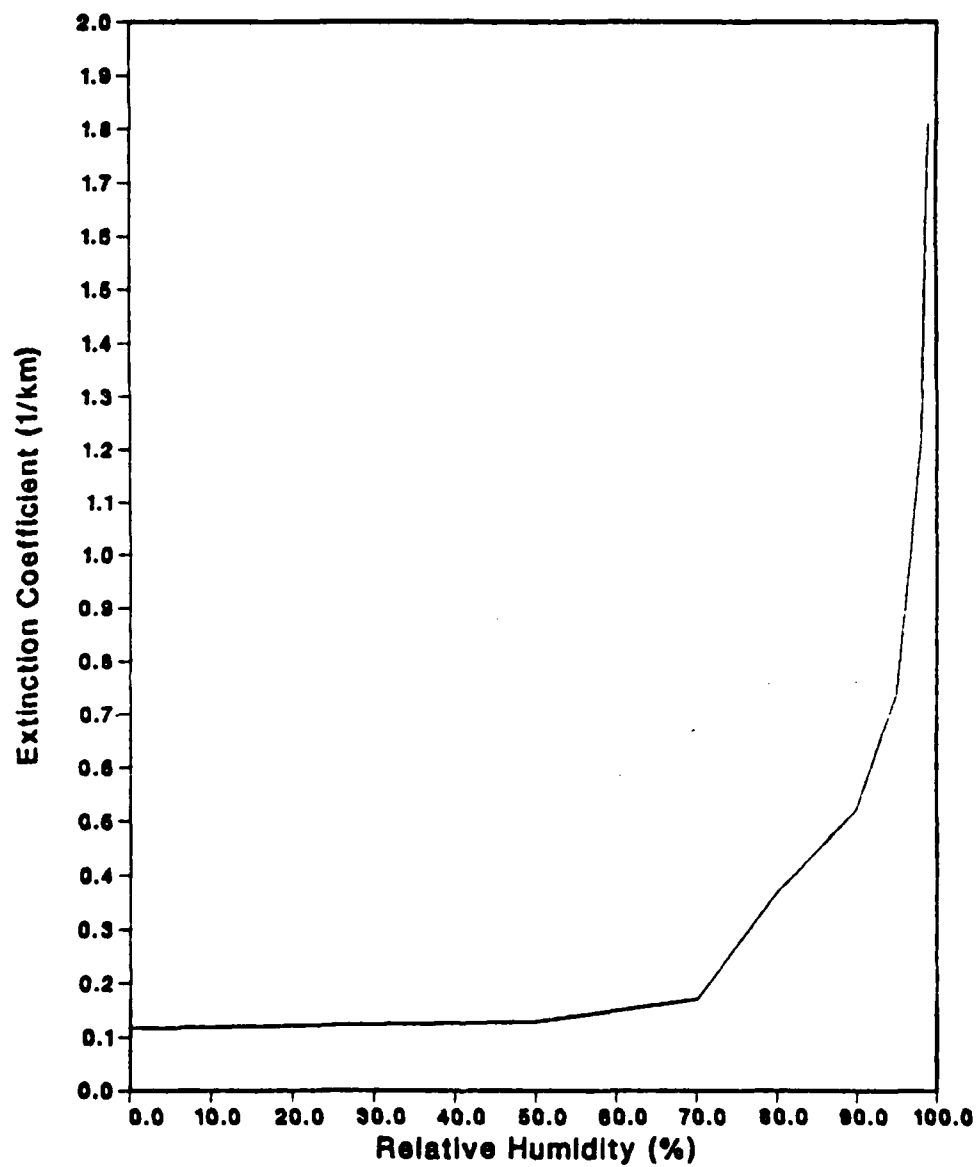


Fig. 3.9 Monotonic behavior of extinction coefficient for marine model from Eqn. 2.2.

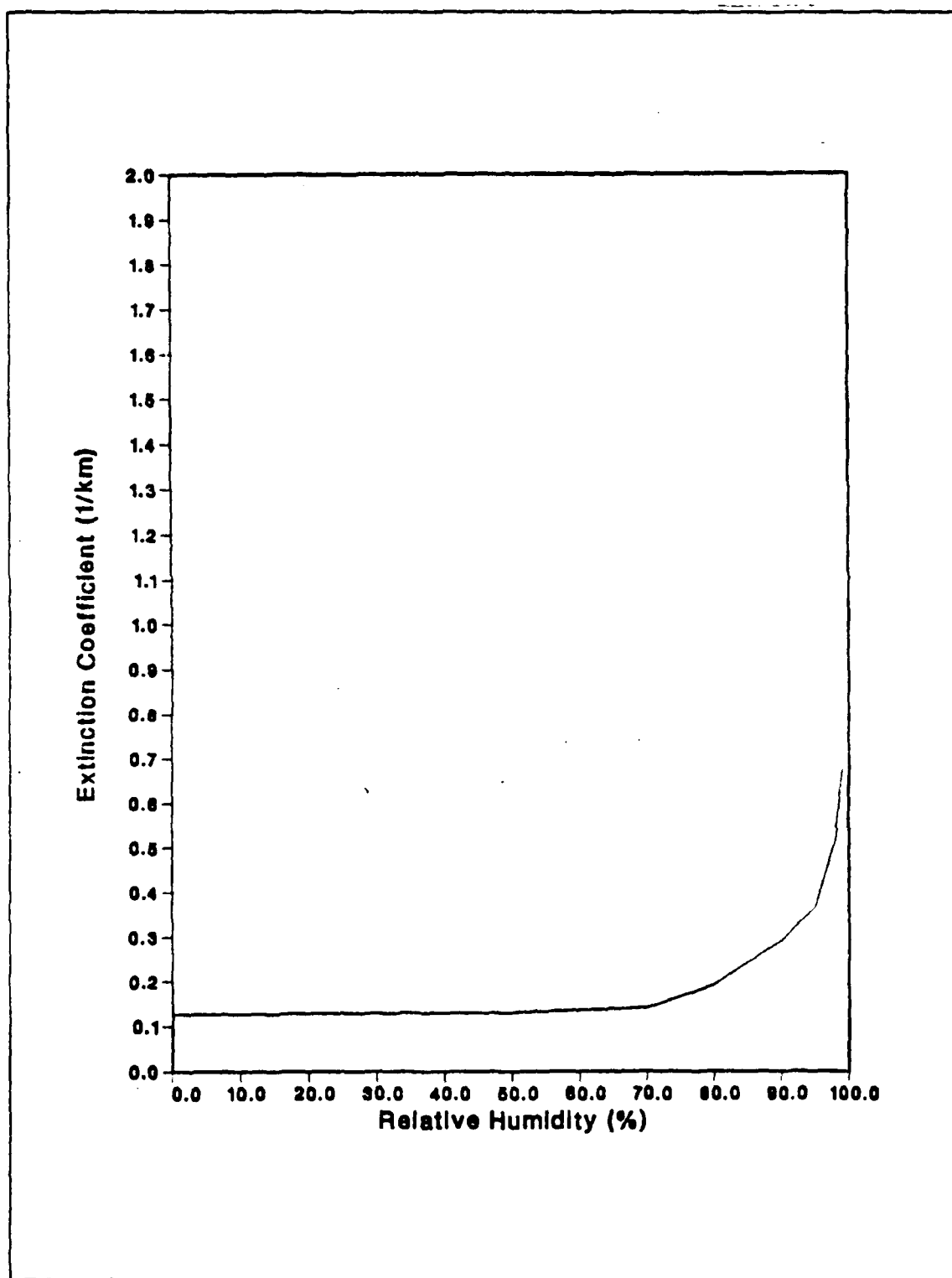


Fig. 3.10 Monotonic behavior of extinction coefficient for rural models from Eqn. 2.2.

IV. RESULTS AND DISCUSSION

After developing a technique to estimate extinction values in the infrared wavelengths from values in the visible and near-infrared, it is necessary to test its limits and sensitivity to several parameters that are included in the model. Five tests were designed with this purpose. The first test is a basic analysis of the technique itself in the retrieval of the particle size distribution. Two of the tests study how variations in the input parameters, extinction coefficient and relative humidity affect the estimated value. The fourth test looks at how deviations from the model size distributions affect the estimated extinction values. The last test compares how an extinction obtained from a three-mode particle size distribution compares to an extinction calculated from a model which assumes a two-mode particle size distribution.

A. BASIC RETRIEVAL ANALYSIS

The first test examines the error associated with the retrieval of a "perfect" satellite estimate of extinction after use of the interpolating technique. The procedure consists of the following steps:

1. Calculate an initial extinction values at 0.63 and 0.86 μm . for a given TN, N2 and RH.
2. Input extinction values into the first portion of the model to retrieve TN and N2 which describe the particle size distribution.
3. Input TN and N2 into the second section of the model to obtain an estimate of the extinction values for all four wavelengths of interest: 0.63, 0.86, 3.75 and 11.00 μm
4. Calculate the error from:

$$\text{error} = 100(\beta_{\text{ext estimated}} - \beta_{\text{ext initial}}) / \beta_{\text{ext initial}} \quad (4.1)$$

5. The procedure is done for both the marine and rural cases.

The basic retrieval test for the marine case was run with values of TN and N2 set to 3,500 cm^{-3} and 0.035 respectively. In the rural case TN was set to 12,000 cm^{-3} and N2 to 0.000175. Humidity values of 25, 50, 75, 85, 96, 98 and 99% were used. Relative humidity values of 25, 75 and 85% needed interpolation by the model. As seen from the results in Table 3 the error associated with the retrieval technique is less than 2.5% for relative humidity values less than 99%. However, this value increases as

the number of parameters that need to be interpolated increases. With all parameters interpolated, the error is still less than 10%. A larger error at the higher humidities was expected because this is where extinction changes the most as shown in Figs. 3.9 and 3.10. The larger error at a relative humidity value of 25% is probably due to the fact that the interpolation for this value occurs over a large range, between 0 and 50% whereas at the higher humidities the difference is 10% or less. The error associated with a relative humidity value of 50% was the lowest and uses an uninterpolated matrix at a relative humidity where there is very little variation in extinction. This shows that the error due to interpolation could be lowered by decreasing the range over which the interpolation is to be performed. This can be accomplished by expanding the number of relative humidity values that are used by the model.

TABLE 3
ERROR ASSOCIATED WITH BASIC RETRIEVAL TECHNIQUE

a. MARINE MODEL

RH(%)	RETRIEVAL ERROR(%)	
	3.75 μ m	11.00 μ m
25	1.9	2.1
75	-0.2	-0.2
96	0.7	0.7
98	1.9	1.9

b. RURAL MODEL

RH(%)	RETRIEVAL ERROR(%)	
	3.75 μ m	11.00 μ m
0	0.6	0.8
50	0.1	0.7
85	1.8	1.5
99	6.5	6.5

B. EXTINCTION ERROR ANALYSIS

The second test evaluated the sensitivity of the technique to errors in the extinction values used as inputs. Several assumptions were made, as discussed in Chapter II, for obtaining the initial input extinction value from satellite radiance

measurements. Therefore, the extinction coefficient estimates may have significant errors. The test consisted of assuming the initial extinction value is in error by ± 5 , 10, 20%. The procedure was as follows:

1. For a given TN, N2, and RH, calculate β_{ext} at the four wavelengths of interest.
2. Using the value obtained in step (1) calculate a β_{ext} value at 0.63 and 0.86 μm that is off by $\pm 5\%$.
3. Input above value into the first section of the model to obtain a retrieved TN and N2.
4. Input the retrieved TN and N2 value into the second portion of the model to obtain an estimated extinction value at 3.75 and 11.00 μm .
5. Calculate the error as discussed in IV. A.
6. Repeat procedure for ± 10 and $\pm 20\%$.

The marine model was run for a TN value of $3,500 \text{ cm}^{-3}$ and an N2 value of 0.035. For the rural case TN was set at $15,500 \text{ cm}^{-3}$ and N2 at 0.000135, using relative humidities of 25, 75, 96 and 98%. The extinction values were then varied by ± 5 , 10, 20 and 25%, as explained above for each humidity value. Table 4 shows the error associated with a variation in RH on an estimated extinction coefficient value at near-infrared and infrared wavelengths. As seen from the results, the magnitude of the error is basically determined from the accuracy of the extinction value within a couple of percentage points. This was expected since the retrieval method itself is accurate to better than 2% for most relative humidities. Slightly larger errors (3-5%) for the rural model are observed for a humidity value of 98% where the value of extinction grows exponentially as seen in Fig. 3.10. The larger errors for the rural model at RH = 98% are observed for extinction errors of 20% or larger. This follows the inherent error of the retrieval technique at this humidity. Thus error in the predicted extinction is less than 3% for all humidities for both models after considering the initial extinction error and the error inherent in the retrieval technique.

C. RELATIVE HUMIDITY ERROR ANALYSIS

Several assumptions were made in the development of the model for estimating extinction coefficients relating to relative humidity. The first assumption deals with the fact that relative humidity varies in the marine atmospheric boundary layer (MABL) with height. Relative humidity generally increases from the surface to the top of the MABL then decreases drastically to near zero at the top of the inversion layer as previously shown in Fig. 3.1. This model assumes input of an average value of relative humidity. The second assumption is that the relative humidity value is known. It may

TABLE 4
ERROR ASSOCIATED WITH UNCERTAINTY IN EXTINCTION
VALUE

a. MARINE MODEL

RH(%) %ERROR ON β_{ext}		PREDICTED ERROR(%)			
		3.75 μ m		11.00 μ m	
25	± 5	7.1	- 3.2	6.7	- 3.1
25	± 10	11.8	- 8.3	11.9	- 8.3
25	± 20	22.3	-18.4	22.2	-18.6
25	± 25	27.4	-23.7	27.3	-23.7
75	± 5	4.8	- 5.3	4.9	- 5.3
75	± 10	9.8	-10.2	9.8	-10.2
75	± 20	19.5	-20.1	19.8	-20.2
75	± 25	24.5	-25.1	24.7	-25.0
96	± 5	5.7	- 4.4	5.8	- 4.3
96	± 10	10.7	- 9.4	10.8	- 9.3
96	± 20	--	-19.5	--	-19.4
96	± 25	--	-24.5	--	-24.3
98	± 5	7.0	- 3.2	7.0	- 3.2
98	± 10	12.1	- 8.3	12.1	- 8.3
98	± 20	22.3	-18.5	22.3	-18.5
98	± 25	27.4	-23.7	27.4	-23.6

b. RURAL MODEL

RH(%) %ERROR ON β_{ext}		PREDICTED ERROR(%)			
		3.75 μ m		11.00 μ m	
25	± 5	5.4	- 5.4	5.8	- 5.8
25	± 10	11.5	-10.9	11.5	-10.8
25	± 20	19.4	-18.8	19.4	-19.4
25	± 25	24.8	-24.2	25.2	-24.5
75	± 5	5.3	- 4.9	5.6	- 4.3
75	± 10	10.2	- 9.7	10.5	- 9.3
75	± 20	20.4	-19.9	20.4	-19.8
75	± 25	25.2	-25.2	25.9	-24.7
96	± 5	3.3	- 8.9	3.2	- 8.7
96	± 10	8.4	-13.6	8.1	-13.6
96	± 20	18.2	-23.6	18.0	-23.5
96	± 25	23.1	-28.3	22.9	-28.4
98	± 5	9.7	- 7.8	9.5	- 7.3
98	± 10	10.2	- 6.5	14.9	- 6.6
98	± 20	25.4	-16.8	25.3	-16.9
98	± 25	29.9	-22.4	29.7	-22.4

be obtained from in situ measurements or in the future, perhaps, from satellite data (Kren, 1987). Changes in the relative humidity change the shape of the particle size distribution as shown in Fig. 2.3. In this study it was assumed that estimates of relative humidity value can be obtained within a certain degree of accuracy ($\pm 5\%$). A series of commercial humidity sensors were tested under laboratory conditions (Muller and Beekman, 1987). Test results show that for some of the sensors accuracies of 95% or better were achieved. Therefore, the test performed was in keeping with the accuracy reported for humidity sensors.

The procedure for this study consisted of the following:

1. For a given TN, N2 and RH, calculate the initial extinction: for example enter an 'observed' (the real RH value) RH = 65%.
2. Use the extinction values obtained for 0.63 and 0.86 μm and input into the first section of the model. Enter an 'assumed' RH value that is $\pm 5\%$ (for example enter RH = 70%) to obtain TN and N2.
3. Enter TN and N2 from above and the same RH value used in step 2 into the second portion of the model to obtain the estimated extinction. Following our example, enter an 'assumed' (due to errors in the instrument that measures RH) RH = 70%.
4. Calculate error as discussed in IV. A.
5. Repeat for -5% . Also repeat for different RH values for both marine and rural models.

The marine case was run for TN set to $3,500 \text{ cm}^{-3}$ and N2 set to 0.0175 whereas the rural case values were $15,000 \text{ cm}^{-3}$ and 0.000135 respectively. Table 5 shows that, for the marine model, a 5% error in relative humidity values give rise to a range of 5-14% errors in β_{ext} at the near-infrared and infrared wavelengths. In the rural model a similar error in RH gives rise to estimated β_{ext} values being in error from 9-31%. As seen in Table 5, the rural model is more sensitive to errors in relative humidity at 11.00 μm wavelength than the marine model. Recall that extinction coefficients are a function of the particle size distribution. At 0.63 and 0.86 μm the satellite data contain more information regarding the first mode in the rural case in contrast to more information on the second mode for the marine case. This can be seen if a vertical line is drawn for radii of 0.63 and 0.86 μm on Figs. 4.1 and 4.2 until they intersect the solid line. The slope of the line at the point of intersection for the marine case is more dependent on changes in the shape of the second mode. Thus, a decrease in the slope infers a larger number of particles at the larger radii. As relative humidity increases the number of particles at the larger radii increases. At the higher wavelengths these larger particles contribute more to the extinction coefficient since they are more heavily

weighted. Since the information in β_{ext} about the second mode is limited in the rural model, a larger error is expected as observed in Table 5.

D. PARTICLE SIZE DISTRIBUTION ERROR ANALYSIS

The next study investigates the error associated with errors in the particle size distribution obtained by changing the average radius of the second mode. The particle size distribution can be altered by changes in the relative humidity, as was shown in III. C. The distribution can also be changed by changing the average radius of the particles for the second mode, r_2 , of Eqn. 2.3. The second mode of the marine case was the only one tested since it is known that it consists of sea spray particles, which are more likely to vary in size due to variations in the wind. Changing r_2 by $\pm 20\%$, as seen on Fig. 4.3, moves the center of the second mode. The model was run with TN set to $4,000 \text{ cm}^{-3}$ and N2 set to 0.02. The procedure is as follows:

1. Change r_2 value for a given relative humidity value in the prediction model by $\pm 5\%$. Calculate the initial extinction values representing a non-ideal particle size distribution. Reset the parameters.
2. Enter extinction values into the first portion of the model to obtain values for TN and N2.
3. Enter TN and N2 into the second section of the model to obtain the predicted extinction values.
4. Calculate error as discussed in IV. A.
5. Repeat for $\pm 10\%$ and $\pm 20\%$ r_2 variations in the marine case only.

As we increase r_2 we change the distribution by increasing the number of particles with a larger radii. Table 6 shows that as we increase the variation in r_2 the error associated with the positive deviations at $\lambda = 3.75 \text{ }\mu\text{m}$ increases from 0.5 to 10% while the error associated with the negative deviations increased from 6 to 25%. For $\lambda = 11.00 \text{ }\mu\text{m}$ the error associated with the positive deviations increased from 0 to 20% whereas for negative deviations the error increased from 9 to 41%. The error is greatest for negative deviations at the 11.00 μm wavelength. Again, at the 0.63 and 0.86 μm wavelengths the extinction efficiency function weighs the larger particles more heavily for higher wavelengths as shown in Figs. 2.1 and 2.2. If a vertical line is drawn to the solid line for $\lambda = 0.63$ and 0.86 μm , as seen in Fig. 4.3, it can be shown that more information is contained in β_{ext} at 0.63 and 0.86 μm about the second mode for positive deviations. The net result is that the error is larger for the -20% r_2 change.

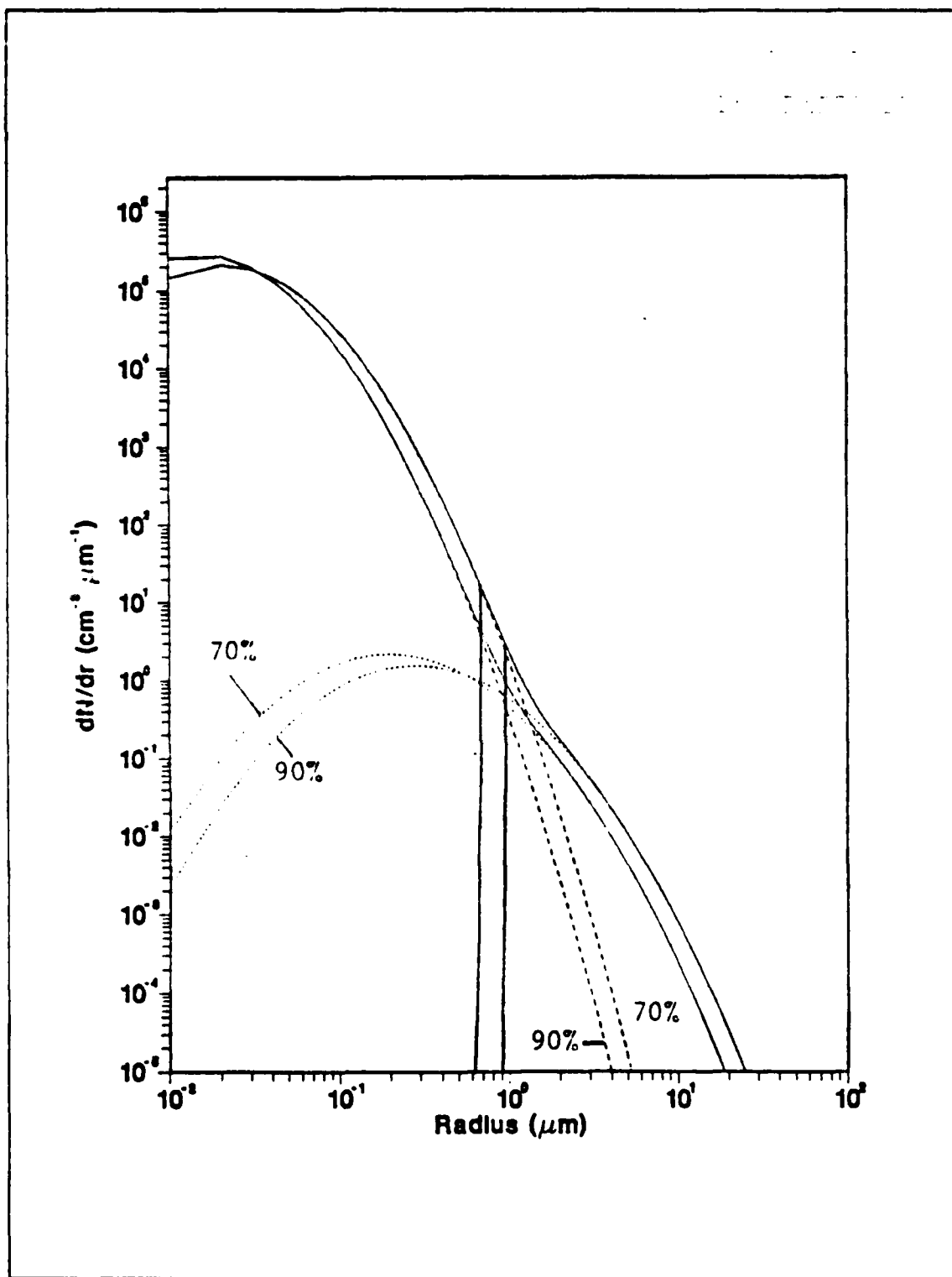


Fig. 4.1 Effect on the distribution of marine particles by changing RII by 20%. Vertical lines at Q_{ext} peak for $\lambda = 0.63$ and $0.86 \mu\text{m}$. Sum of modes 1 & 2 (solid), mode 1 (dashed), mode 2 (dot).

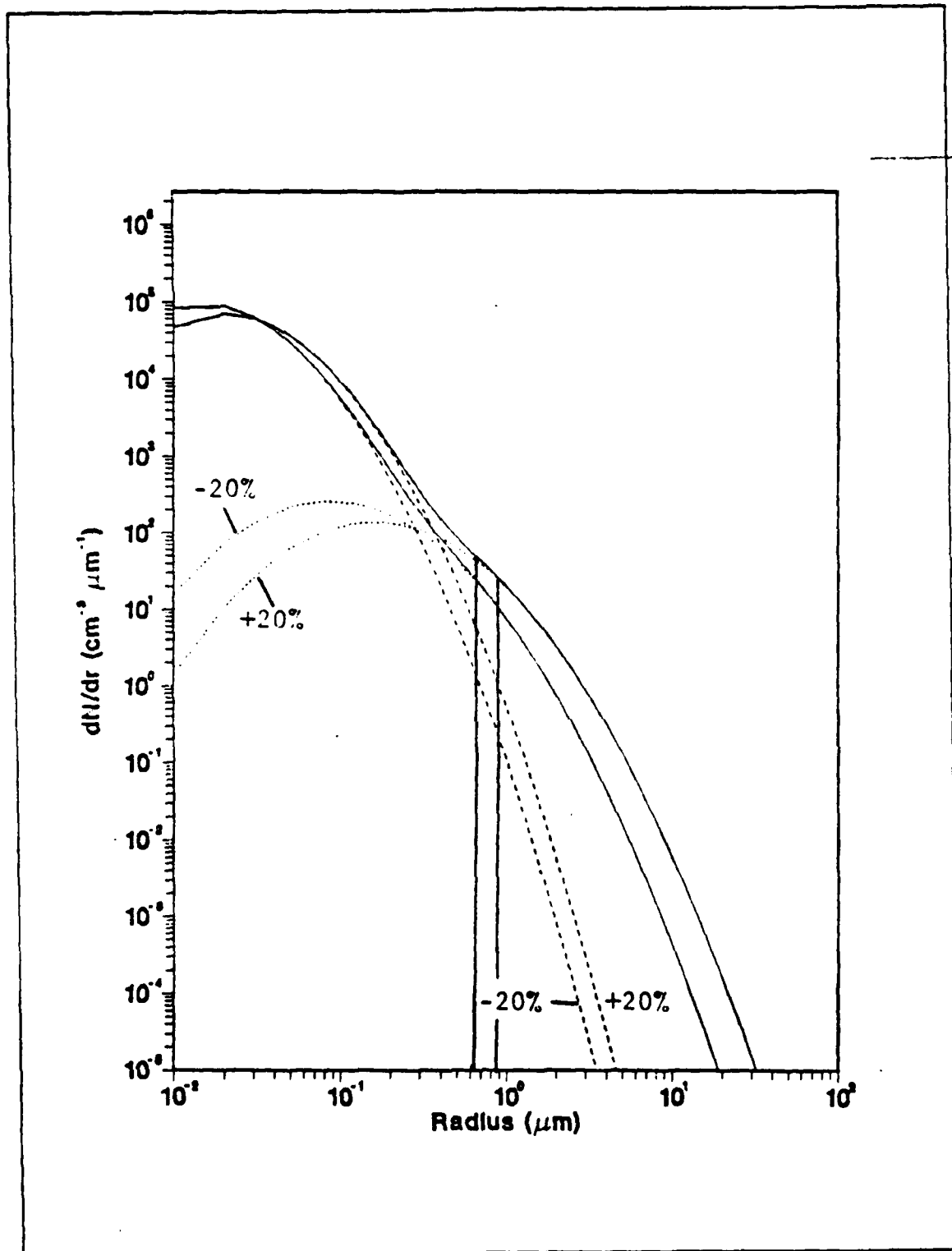


Fig. 4.2 Effect on the distribution of rural particles by changing RH by 20%. Vertical lines at Qext peak for $\lambda = 0.63$ and $0.86 \mu\text{m}$. Sum of modes 1 & 2 (solid), mode 1 (dashed), mode 2 (dot).

TABLE 5
RELATIVE HUMIDITY SENSITIVITY STUDY

a. MARINE MODEL

RH(%)		PREDICTED ERROR(%)	
OBS	ASSUMED	3.75 μ m	11.00 μ m
65	70	11.8	9.0
75	70	-10.2	-11.8
85	90	8.6	12.6
95	90	-5.3	-13.5

b. RURAL MODEL

RH(%)		PREDICTED ERROR(%)	
OBS	ASSUMED	3.75 μ m	11.00 μ m
65	70	21.7	16.2
75	70	17.2	23.4
85	90	13.3	9.1
95	90	28.6	30.8

E. THREE-MODE PARTICLE SIZE DISTRIBUTION ERROR ANALYSIS

The model for the estimation of extinction coefficients assumes that the marine particle distribution arises from particles of a continental and marine origin. In conditions of high winds this is altered by the introduction of larger size particles into the marine boundary layer. As the wind speed increases above 9 m/s, waves crest and particles are ejected into the atmosphere (Monahan *et al.*, 1983). These particles have an average radius of 2 μ m and comprise the third mode of the particle size distribution (Gathman, 1983). The purpose of this test was to examine the effect of input of an extinction coefficient obtained from a variable wind regime and estimate extinction values using the assumed two-mode model. The model for the estimation of extinction coefficient was modified to allow addition of a third wind-dependent mode represented by variable A3 as shown previously in Fig. 2.4. The values of A3 equal to 1.0, 0.5 and 0.1 were taken to represent the production of 10 μ m particles at wind speeds of approximately 31, 27, and 15 m/s respectively. The shape of A3 is described by: $A3 = 10\exp(.06 \times \text{wind speed} - 2.8)$ and is a modification of the Navy Aerosol Model

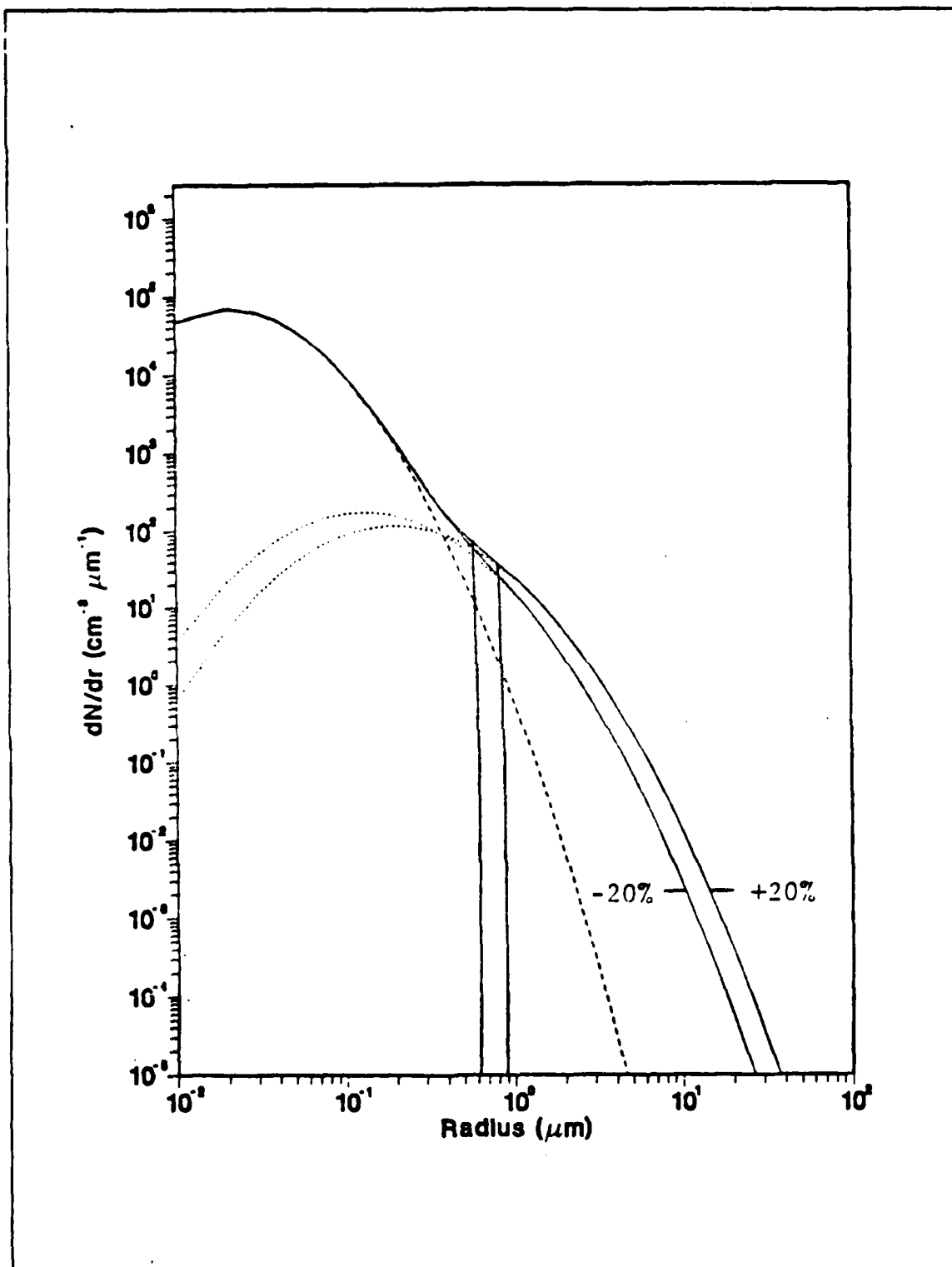


Fig. 4.3 Effect of changing r_2 on the distribution of marine particles by $\pm 20\%$. Vertical lines at Q_{ext} peak for $\lambda = 0.63$ and $0.86 \mu\text{m}$. Sum of modes 1 & 2 (solid), mode 1 (dashed), mode 2 (dot).

TABLE 6
PARTICLE SIZE DISTRIBUTION SENSITIVITY STUDY

MARINE MODEL		PREDICTED ERROR(%)			
RH(%)	R2(%)	3.75 μ m		11.00 μ m	
50	± 5	0.5	8.7	0.0	11.8
50	± 10	-4.1	18.2	-9.7	24.5
50	± 20	-10.5	25.0	-20.6	40.5
70	± 5	0.7	8.4	-2.1	11.0
70	± 10	-4.0	17.5	-9.0	22.9
70	± 20	-10.0	22.7	-19.0	35.8
85	± 5	1.3	6.4	-1.3	9.2
85	± 10	-1.1	13.6	-6.1	19.4
85	± 20	-8.2	10.7	-17.1	14.0
90	± 5	--	8.8	--	11.9
90	± 10	--	14.3	--	21.0
90	± 20	-5.0	21.5	-4.8	36.5

(Gathman, 1983).¹ The model was run with TN set at 4,000 cm⁻³ and N2 set at 0.02 for relative humidity values of 70 and 90% and TN was set at 4,135 cm⁻³ and N2 at 0.0135 for relative humidity values of 60 and 85%. Different parameters were selected to test the sensitivity when matrices were not interpolated. The procedure was as follows:

1. Obtain an initial extinction value of extinction for a given TN, N2, RH and A3 value. For the first run set A3 to 1.0.
2. Enter the extinction coefficients into the first section of the prediction model to retrieve a value for TN and N2.
3. Enter TN, N2, RH and an A3 value of 0.0, which reverts the program back to a two-mode distribution, into the second portion of the prediction model to obtain the predicted extinction values at 3.75 and 11.00 μ m.
4. Calculate the error as discussed in IV. A.
5. Repeat for A3 values of 0.5 and 0.1. Also repeat for several relative humidity values for the marine model only.

¹From H. Hughes by personal communication, present affiliation: Ocean and Atmospheric Sciences Division, Naval Ocean Systems Center, San Diego, CA 92152-5000.

With the addition of a third mode we observe in Table 7 that the error is greatest at the higher wind speed, up to 82% for $A_3=1$ and $\lambda=11.00 \mu\text{m}$ and up to 39% at $\lambda=3.75 \mu\text{m}$. Results show that the errors decreased as relative humidity values increase. The addition of more particles at the higher radii for lower RH values influences the result more and thus the higher error at the lower RH values. Also, since the higher radii are weighted more by the extinction efficiency function for the higher wavelength a higher error is observed at $11.00 \mu\text{m}$. There is a slight increase in error at 60% RH due to the added interpolation step over a 20% range of relative humidity. The interpolation error is not observed at 85% RH since the interpolation is over a 10% spread and the error associated with the introduction of the third mode dominates.

TABLE 7
EFFECT OF A THREE-MODE PARTICLE SIZE DISTRIBUTION

MARINE MODEL

RH(%)	A3	PREDICTED ERROR(%)	
		3.75 μm	11.00 μm
60	1.0	-39.0	-81.7
60	0.5	-30.2	-75.8
60	0.1	-7.1	-47.2
70	1.0	-30.2	-75.5
70	0.5	-22.3	-67.0
70	0.1	-4.0	-33.1
85	1.0	-1.3	-32.8
85	0.5	-1.3	-32.8
85	0.1	8.0	-3.5
90	1.0	-3.7	-34.5
90	0.5	-1.3	-22.4
90	0.1	-0.1	-5.9

V. CONCLUSIONS AND RECOMMENDATIONS

A method for estimating extinction coefficients in the near-infrared and infrared wavelengths using channels 1 and 2 of the NOAA-7 AVHRR was developed. The model consists of two sections. Input of the type of aerosol model (marine or rural) and the effective relative humidity value for the boundary layer defines the average mode radius. Input of the extinction coefficient at 0.63 and 0.86 μm determine the magnitude of the retrieved parameters, TN and N2, necessary to describe the distribution of aerosols. The second section uses these values and the effective relative humidity value for the boundary layer to estimate the extinction coefficients at 3.75 and 11.00 μm .

Five tests were developed to determine the limits and sensitivity of the model. The first test examined the error associated with the retrieval of a 'perfect' satellite estimate of extinction. Given an initial value of extinction at 0.63 and 0.86 μm for a given TN and N2, results show that the retrieval error is the smallest at the middle humidity values where the extinction coefficient, as a function of relative humidity, changes the least and interpolation occurs over a relatively small range (10% spread).

Results for the second test show that the models' accuracy is basically determined from the accuracy of the input extinction coefficient values. Error in the predicted extinction is less than 3% after considering the error in input extinction for all humidities tested and for both models.

Relative humidity affects the distribution of large radii particles in the marine atmospheric boundary layer. A 5% error in the value of the relative humidity for the area of interest will lead to errors as high as 14% for the marine model and 31% for the rural model in the estimated extinction coefficient values at the longer wavelengths. This test shows that errors in relative humidity affect the rural model the most, since the information contained in the second mode is more limited for the rural model for a given relative humidity.

The particle size distribution can also be changed by increasing the average size of the particles in the boundary layer. Thus changes in the mode radius by 5, 10, 20% will result in an error in the estimated extinction coefficient value of up to 12, 24 and 40% respectively. The highest errors are for calculations at the 11.00 μm wavelengths since the extinction efficiency function weighs the larger radii the most.

The last test evaluates the performance of a two-mode particle size distribution model against the Navy aerosol three-mode model. With the addition of a third mode, we observe that the error decreases as the wind speed decreases. Since the third mode contains very large particles, the error is highest for estimates at 11.00 μm as expected.

Three general conclusions can be made from this study. First, estimates of extinction at infrared wavelengths rely heavily on the accuracy of the input extinction coefficient values at 0.63 and 0.86 μm . Therefore, care must be exercised in obtaining the best possible value of extinction from satellite estimates of optical depth and NOLAPS estimate of boundary layer depth. The second is that extinction is dependent on particle size distribution and thus the shape of the distribution used in the model will affect the estimated value directly. And finally, factors affecting the particle size distribution, such as relative humidity and wind speed, must be taken into account.

It must be noted here that the model as it stands now is limited to certain TN and N2 values. To be used operationally these parameters and the associated extinction matrices would have to be expanded. Error in the interpolating technique can be decreased by increasing the number of relative humidity values that are used in the model. Also, due to large particles being generated by high winds, the model should be modified to allow for variable winds similar to the Navy aerosol model. Lastly, methods for estimation of relative humidity, to accuracies of 95% or better, need to be developed for meteorological satellites to facilitate measurement of relative humidity in remote areas and thus provide better input into the model.

LIST OF REFERENCES

- Burk, S. D., and W. T. Thompson, 1982: Operational Evaluation of a Turbulence Closure Model Forecast System. *Monthly Weather Review*, 110, 1535-1543.
- Durkee, P. A., 1984: The Relationship Between Marine Aerosol Particles and Satellite-Detected Radiance. Ph. D. Dissertation, Colorado State University, Fort Collins, CO, 124 pp.
- Durkee, P. A., D. R. Jensen, E. E. Hindman and T. H. Vonder Haar, 1986: The Relationship Between Marine Aerosol Particles and Satellite-Detected Radiance. *Journal of Geophysical Research*, 91, 4063-4072.
- Durkee, P. A., 1987: Aerosol Characteristics Inferred from DualWavelength Radiance Measurements. Submitted to *Journal of Geophysical Research*.
- Fairall, C. W., and K. L. Davidson, 1986: Dynamics and Modeling of Aerosols in the Marine Atmospheric Boundary Layer. In *Oceanic Whitecaps and Their Role in Air-Sea Exchange Processes*, Edited by E. C. Monahan and G. MacNiocaill. D. Reidel Publishing Company, 3300 AA Dordrecht, Holland.
- Fritsch, F. N., 1982: Piecewise Cubic Hermite Interpolation Package Mathematics and Statistics Division, Lawrence Livermore National Laboratory, Livermore, CA. 52 pp.
- Gathman, S. G., 1983: Optical Properties of the Marine Aerosol as Predicted by a BASIC Version of the Navy Aerosol Model. NRL Memorandum Report 5157, Naval Research Lab, Washington, D. C., 31 pp.

- Gerber, H., 1985: Infrared Aerosol Extinction From Visible and Near-Infrared Light Scattering. *Applied Optics*, **34**, 4155-4166.
- Kneizys, F. X., E. P. Shettle, W. O. Gallery, J.H. Chetwynd, Jr., L. W. Abreu, J. E. A. Selby, S. A. Clough and R. W. Fenn, 1983: Atmospheric Transmittance/Radiance Computer Code LOWTRAN 6. AFGL-TR-83-0187, Environmental Research Papers, No. 846, Air Force Geophysics Laboratories, Hanscom AFB, MA, 200 pp.
- Kren, R., 1987: An Estimation of Marine Boundary Layer Depth and Relative Humidity with Multispectral Satellite Measurements. M. S. Thesis, Naval Postgraduate School, Monterey, CA. In progress.
- McCartney, E. J., 1976: *Optics of the Atmosphere: Scattering by molecules and Particles*. J. Wiley, New York, 408 pp.
- Mitchell, W. F., S. Englander, J.J. Ferrari and J. Bohse, 1982: Environmental Impact on Naval Weapon System Development Volume II. Report N00019-81-C-0144 Department of the Navy, Naval Air Systems Command, Air 370G, Washington, D. C. 20361, AFGL-TR-79-0214 Air Force Geophysics Laboratories, Hanscom AFB, MA, 01731, 256 pp.
- Monahan, E. C., D. E. Spiel and K. L. Davidson, 1983: Model of Marine Aerosol Generation Via White Caps and Wave Disruption. Ninth Conference on Aerospace and Aeronautical Meteorology, Omaha, NE, 6-9 June 1983.
- Muller, S. H., and P. J. Beekman, 1987: Commercial Humidity Sensors for Use at Automatic Weather Stations: A Laboratory Test. Sixth Symposium Meteorological Observations and Instrumentation, New Orleans, LA, 12-16 January 1987.

Shettle, E. P., and R. W. Fenn, 1979: Models for the Aerosols of the Lower Atmosphere and the Effects of Humidity Variations on Their Optical Properties. AFGL-TR-79-0214 Air Force Geophysics Laboratories, Hanscom AFB, MA, 94 pp.

Whitby, K. T., and Cantrell, B., 1975: Atmospheric Aerosols - Characteristics and Measurements. International Conf. on Environmental Sensing and Assessment. Las Vegas, NV, 14-19 September 1975.

INITIAL DISTRIBUTION LIST

	No. Copies
1. Defense Technical Information Center Cameron Station Alexandria, VA 22304-6145	2
2. Library, Code 0142 Naval Postgraduate School Monterey, CA 93943-5002	2
3. Chairman (Code 63Rd) Department of Meteorology Naval Postgraduate School Monterey, CA 93943-5000	1
4. Chairman (Code 68Tm) Department of Oceanography Naval Postgraduate School Monterey, CA 93943-5000	1
5. Professor P. A. Durkee (Code 63De) Department of Meteorology Naval Postgraduate School Monterey, CA 93943-5000	6
6. Professor C. Wash (Code 63Wx) Department of Meteorology Naval Postgraduate School Monterey, CA 93943-5000	1
7. Professor K. L. Davidson (Code 63Ds) Department of Meteorology Naval Postgraduate School Monterey, CA 93943-5000	1
8. Professor R. Franke (Code 53Fe) Department of Mathematics Naval Postgraduate School Monterey, CA 93943-5000	1
9. LT Margarita Garcia de Quevedo U.S. Naval Oceanography Command Center Joint Typhoon Warning Center COMNAVMARIANAS Box 12 FPO San Francisco 96630-2926	1
10. Director Naval Oceanography Division Naval Observatory 34th and Massachusetts Avenue NW Washington, DC 20390	1
11. Commander Naval Oceanography Command NSTL Station Bay St. Louis, MS 39522	1
12. Commanding Officer Naval Oceanographic Office NSTL Station Bay St. Louis, MS 39522	1

13. **Commanding Officer**
Fleet Numerical Oceanography Center
Monterey, CA 93943-5000 1
14. **Commanding Officer**
Naval Ocean Research and Development Activity
NSTL Station
Bay St. Louis, MS 39522 1
15. **Commanding Officer**
Naval Environmental Prediction Research Facility
Monterey, CA 93943-5000 1
16. **Julie Haggerty**
Naval Environmental Prediction Research Facility
Monterey, CA 93943-5000 1
17. **Chairman, Oceanography Department**
U.S. Naval Academy
Annapolis, MD 21402 1
18. **Chief of Naval Research**
800 N. Quincy Street
Arlington, VA 22217 1
19. **Office of Naval Research (Code 420)**
Naval Ocean Research and Development Activity
800 N. Quincy Street
Arlington, VA 22217 1
20. **Scientific Liason Office**
Office of Naval Research
Scripps Institution of Oceanography
La Jolla, CA 92037 1
21. **Mr. Dale F. Johnson**
Code 206-41
California Institute of Technology
Pasadena, CA 91106 1
22. **Dr. and Mrs. J. L. Garcia de Quevedo**
Carr. 108 #1435
Mayaguez, Puerto Rico 00708-7416 1
23. **Mr. and Mrs. Neil Johnson**
8740 Sardis Road
Matthews, NC 28105 1

END

7-87

DTIC